The cellulose–lignin balance affects the twisted growth of Yunnan pine trunk

kai cui[1], Zirui Liu[1], Jin Li[1], Chengjie Gao[1], and Yingchun Miao[1]

[1]State Key Laboratory of Tree Genetics and Breeding Institute of Highland Forest Science Chinese Academy of Forestry Kunming 650233 PR China

October 10, 2022

Abstract

It is a debate whether trunk twisting belongs to environmental alteration or genetic variation. Through a diallel cross experiment, we first determined that trunk twisting of Yunnan pines was controlled by recessive genes. Anatomical analysis identified that straight and twisty types differed in xylem and phloem. RNA-seq of materials enriched by laser microdissection revealed three genes involved in auxin signal transduction, photosynthesis, and sucrose metabolism, namely *ARF*, *POR*, and *CBH.* These genes were co-expressed at different growth stages of twisty types, and among them, *ARF* is crucial regulating trunk twisting formation. The enzyme activities involved in sucrose metabolism, carbon fixation, and glycolysis were significantly increased after exogenous auxin was added to twisty types. When auxin signal transduction inhibitor (auxinole) and transport inhibitor (TIBA) were added, the plant height and related pathways were more obviously reduced in straight types. *ARF* can not only downregulate *POR* to block chlorophyll synthesis but also allows abundant sucrose to synthesize cellulose. Nevertheless, due to downregulated *CBH* expression and abnormal cellulolysis, cellulose accumulates and the lignin content decreases, eventually making the trunk highly prone to twisted growth. This study suggests that *ARF* can be vital in trunk shape screening during the early growth of Yunnan pines.

The cellulose–lignin balance affects the twisted growth of Yunnan pine trunk

Zirui Liu, Jin Li, Chengjie Gao, Yingchun Miao, Kai Cui*

State Key Laboratory of Tree Genetics and Breeding, Institute of Highland Forest Science, Chinese Academy of Forestry, Kunming 650233, PR China

* Corresponding author (cuikai@caf.ac.cn)

Phone: 86-871-63860026; Fax: 86-871-63860027

ABSTRACT

It is a debate whether trunk twisting belongs to environmental alteration or genetic variation. Through a diallel cross experiment, we first determined that trunk twisting of Yunnan pines was controlled by recessive genes. Anatomical analysis identified that straight and twisty types differed in xylem and phloem. RNA-seq of materials enriched by laser microdissection revealed three genes involved in auxin signal transduction, photosynthesis, and sucrose metabolism, namely *ARF* ,*POR* , and *CBH.* These genes were co-expressed at different growth stages of twisty types, and among them, *ARF* is crucial regulating trunk twisting formation. The enzyme activities involved in sucrose metabolism, carbon fixation, and glycolysis were significantly increased after exogenous auxin was added to twisty types. When auxin signal transduction inhibitor (auxinole) and transport inhibitor (TIBA) were added, the plant height and related pathways were more obviously reduced in straight types. *ARF* can not only downregulate*POR* to block chlorophyll synthesis but also allows abundant sucrose to synthesize cellulose. Nevertheless, due to downregulated*CBH* expression and abnormal

cellulolysis, cellulose accumulates and the lignin content decreases, eventually making the trunk highly prone to twisted growth. This study suggests that *ARF* can be vital in trunk shape screening during the early growth of Yunnan pines.

KEYWORDS

Trunk, twisted growth, controlled crossing, RNA-seq, IAA, cellulose

1 INTRODUCTION

Plants usually grow in a linear or circumferential orientation; however, some plants show twisted (Kerwin, 2021), spiral, and circled growth (Zheng et al., 2018). These phenotypic traits are alterations caused by increased environmental selection pressure (Max et al., 2021; Alexandra et al., 2019) or heritable variations (Guo et al., 2022). Some genes involved in twisted growth have been identified using model plants, including*SmSPR1* (Liu et al., 2021), *WAVY* (Masashi et al., 2010), *spiral1* , *spiral2* (Stéphane et al., 2019),*lefty1* , *lefty2* (Siripong et al., 2002), and *CSI1*(Martin et al., 2012). These genes mainly play a regulatory role in microtubule motility. Microtubule and microfiber development is the driving force for cell development (Li et al., 2012). In plants, twisted growth is tightly linked to microtubule development, cellulose biosynthesis (Collings et al., 2021), cell wall architecture (Joanna & Joseph, 2019), and organ biomechanics that control organ growth and morphogenesis (Emonet & Hay, 2022). Moreover, adjacent cells tend to coordinate plant growth through the connectivity of the cell wall, implying that all cells rotate in-phase around the organ axis when twisting an axial organ (Renate et al., 2011). Wang et al. (2021) discovered that ectopically expressed *GhIQD14* , a protein localized to microtubules in *Arabidopsis* , causes twisting of organs such as seedlings, trichomes, rosette leaves, and capsules. By constructing a model, Chakraborty et al. (2021) modeled the expansion force, external force received during plant cell growth, and the interaction between forces during cell wall expansion. They argued that the handedness of twisting cell growth depends on external torque and intrinsic characteristics of the cell wall. According to them, cells produce left-handed spirals by "default" in a sense.

Some studies have investigated the stem twisting phenomenon in woody plants. For example, Shavnin (2018) noticed trunk twisting in both*P. sylvestris* and *Picea obovata* and found that the twisting direction in the second year was likely to be the opposite of the previous year. On the basis of results of the twisting degree and frequency, they reported that forest types and weather conditions were the main contributors to such twisting. They also explained this phenomenon by constructing a morphogenetic model. Liu et al. (2012) proposed that abnormal expression of the cellulose synthase gene*PtCesA8A* in *Populus tomentosa* may induce twisting by reducing stem stiffness. Genetic patterns of trunk twisting were investigated through controlled cross tests on *Corylus avellana*(David & Mehlenbacher, 1996) and *Salix matsudana* (Lin et al., 2007).

Yunnan pine (*Pinus yunnanensis* Franch.) mainly grows in the central Yunnan Plateau and extends to some areas of Tibet, Sichuan, Guangxi, and Guizhou, which are adjacent to Yunnan (Fan et al., 2021). This is a typical plant of the subtropical arid region of western China (Li et al., 2021; Zhang et al., 2021) and is a forest type with the largest extant area in Yunnan Province, accounting for 19.63% of the total forest stands and 14.28% of the forest stock in this province. Thus, Yunnan pine occupies a pivotal position in forestry production (Jerzy et al., 2021) and eco-economic construction in southwest China (Pan et al., 2017). The trunk twisting phenomenon of Yunnan pines has aroused considerable attention, with some studies attributing it to environmental conditions. For instance, by observing the macrostructure and phloem microstructure of the pine bark at different latitudes and altitudes, Wang et al. (2009) concluded that trunk twisting is a manifestation of adaptation of Yunnan pines to the local climate. However, further studies have suggested that twisting of trunk and texture is genetically controlled. The trunk shape of offspring stands mainly relies on seed tree quality, rather than environmental conditions (Zhou et al., 2016, He, 1994). However, due to the limitation of technical means in the previous studies, whether the trunk twisting of Yunnan pines is controlled by environmental or genetic factors remains unclear.

Plant organs consist of multiple cell and tissue types, and essential gene expression changes occurring in specific cells or tissues can be overlooked by isolating RNA from entire organs (Yoshihito et al., 2018). Laser

capture microdissection (LCM) combines microscopy and laser beams to isolate specific tissue or cell types from the sections of a specimen (Robert et al., 2005). LCM has been employed for isolating and analyzing high-quality RNA, terpene synthase enzyme activity, and terpenoid metabolites from resin ducts and cambial zone tissues of white spruce (*Picea glauca*) (Eric et al., 2010). RNA extracted from the phloem (Nina et al., 2014) has also been used to enrich ray parenchyma cells of *Phellodendron amurense*Rupr. (Zheng et al., 2016). LCM has been widely used for plant transcriptome analysis, such as combining LCM with 454 pyrosequencing for transcriptome analysis of maritime pine (*P. pinaster*). Using an adapted protocol for conifer RNA amplification, complementary DNA (cDNA) was synthesized and amplified from tiny amounts of total RNA from LCM samples. This approach significantly improved sequencing quality and facilitated whole gene expression analysis of conifer tissues (Rafael et al., 2014). Goué et al. (2012) isolated ray and spindle cells from poplar cambium cells through LCM. Transcriptome sequencing was performed on these cells to explore regulatory mechanisms underlying wood quality and quantity, thereby providing theoretical information about how to select the best trees and how to cut them without affecting their physiological parameters. Preserving intact plant cell structures is easier with paraffin embedding and sectioning than with frozen sectioning. However, because the process of paraffin section preparation is lengthy, RNA degradation is likely to occur during this period. Using a modified paraffin sectioning method, Verma et al. (2019) enriched cells of an apple bud meristem through LCM of its paraffin sections and extracted high-quality RNA from the enriched cells. Takahashi et al. (2010) designed a serial sectioning method to ensure RNA integrity by shortening time and reducing temperature at each step of traditional paraffin sectioning. Improvement in RNA quality and yield eliminates major obstacles in the widespread use of LCM with high-throughput technologies for plants.

In this study, through artificially controlled pollination experiments, we first confirmed that trunk twisting of Yunnan pines was a heritable variation trait. Then, LCM-enriched xylem and phloem cells were used for transcriptome analysis to screen for differentially expressed genes (DEGs) during the twisting process and explore significantly enriched metabolic pathways. Key genes involved in twisting were further identified using control experiments, qRT-PCR, and physiological and biochemical index measurements to preliminarily reveal the cause underlying twisting in Yunnan pines.

2 MATERIAL AND METHODS

2.1 Plant materials and controlled crossing

According to a complete diallel crossing design, 15-year-old twisty and straight Yunnan pines from the Lufeng Experimental Station of the Institute of Highland Forest Science, Chinese Academy of Forestry (102°12'10", 25deg13'23"), were selected as parents for controlled crossing. In March 2014, mature pollen of Yunnan pines was collected individually from each plant, dried and placed in clean glass bottles, and stored at 4 in a dry place of the laboratory. When the mother tree started blooming in April, *P. yunnanensis* pollen was sprayed on the female strobilus of the mother tree with a syringe, covered with sulfuric acid paper, and tightened. After 2–3 days, the sulfuric acid paper was unraveled and the female strobilus was re-pollinated. During this process, each mother tree was only pollinated with the pollen individually collected from the same plant, and multiple clonal mother trees were pollinated with different paternal pollens. In total, 7–15 female inflorescences were covered in each bag (n = 10 bags) for each cross. To promote fruit setting after hybridization, the paper bags were removed at the end of all male pollen shedding in the mother forest. In December 2016, mature cones were also individually collected from each plant, and seeds of each plant were used as a hybrid combination. Hybrid seeds were uniformly raised in nutrient bags in March 2017 and used for afforestation in the rainy season of 2018 through a randomized block design (a single row of 5 plants and 4 replicates) with a row spacing of 2 m x 3 m. At the end of each year, each tree was investigated to determine the status of trunk twisting and straightening.

A portion of the harvested hybrid seeds was sown in nutrient soil (organic soil: perlite: vermiculite = 2:1:1), cultured (25, 16 h of light: 8 h of dark, 60% humidity) in an artificial climate chamber (PQX-1000, Hongdu, Shanghai), and watered three times a week. After emergence, the trunk shape was assessed weekly. These materials were used for anatomical experiments, microdissection, RNA-seq, and physiological and

biochemical experiments.

2.2 Histological observation

Straight and twisty stem segments of Yunnan pines of ages 30, 60, and 180 days were selected. Stem samples of approximately 0.5-cm^3 volume were fixed in FAA buffer (50 mL of 70% ethyl alcohol, 5 mL acetic acid, 5 mL formaldehyde, 10 mL glycerin, and 25 mL water) for more than 24 h (Hao et al., 2021; Tao et al., 2020), washed, dehydrated, cleared with tert-butyl alcohol and gradient alcohol, and embedded in paraffin. The stem segments were cut into 10-μm sections with a microtome (Leica RM2135). Paraffin around the plant tissues was washed away with ethanol and xylene (Chen et al., 2019). The sections of Yunnan pines were stained with toluidine blue staining solution containing 0.5% borate, mounted in neutral gum, microphotographed using an Olympus IX71 microscope, and micromeasured with a built-in ruler. The images obtained were analyzed; transverse sections of the stem segments of straight and twisty Yunnan pines were observed through scanning electron microscopy (SEM) (PRECIPOINT M8, Germany), and xylem and phloem cell diameters of the stem segments were measured using ImageJ software.

2.3 LCM

Fresh straight and twisty stems of Yunnan pines were snap-frozen in the OCT embedding medium, stored at -20 °C, and sectioned into 15-μm sections by using a freezing microtome (Leica CM1950). The slides with the sections were dried in a desiccator at 4°C for at least 2 h or dried on a 4°C cold metal block in a vacuum chamber (-0.9 bar) for 15 min (Olsen & Krause, 2019). The cryosections were placed on stainless steel slides with PET membranes (Lecia Microsystems, Wetzlar, Germany), and xylem and phloem cells were collected into the caps of nuclease-free 0.2 mL PCR tubes (Axygen, USA) containing the appropriate buffer for RNA and protein extractions using LCM (LMD7000, Lecia, German). The collected cells were snap-frozen in liquid nitrogen and stored at -80degC (Blokhina et al., 2016). During microdissection of multiple tissues from a single cryosection, dissection of one tissue type was completed before beginning to cut the next tissue type to avoid cross contamination of tissue samples. The settings for dissection were as follows: 10x magnification; aperture: 20; power: 45; and speed: 6 (Agusti et al., 2011).

2.4 RNA extraction, library construction, and RNA-seq

For LCM-enriched tissues, total RNA was isolated using the PicoPure RNA Isolation Kit (Thermo Fisher Scientific, Sweden) (Ranjan et al., 2022). Each sample consisted of three independent biological replicates. The quantity and quality of RNA samples were analyzed using a 2100 Bioanalyzer (Agilent Technologies, USA) (Ram et al., 2020). High-quality RNA samples were used to construct cDNA libraries, and the starting RNA material for library construction was total RNA. mRNA with polyA tails was first enriched with oligo (dT) beads, and the resulting mRNA was subsequently randomly interrupted with divalent cations in fragmentation buffer. First-strand cDNA was synthesized in an M-MuLV reverse transcriptase system by using fragmented mRNA as the template and random oligonucleotides as primers, followed by RNA strand degradation with RNaseH. Second-strand cDNA was synthesized from dNTPs in a DNA polymerase I system. The purified double-stranded cDNA was end-repaired, A-tailed, and ligated with sequencing adapters. The cDNA of approximately 370–420 bp was screened using AMPure XP beads and amplified by PCR. The PCR product was purified again with the AMPure XP beads to finally obtain the libraries. Illumina NovaSeq 6000 sequencing (Ye et al., 2020) was performed after pooling different libraries according to the effective concentration and the amount of on-target data. A total of 150-bp paired-end reads were generated. The basic principle of sequencing is sequencing by synthesis. For amplification, four fluorescently labeled dNTPs, DNA polymerase, and adaptor primers were added to the sequenced flow cell. When each sequencing cluster extended the complementary strand, each fluorescently labeled dNTP released the fluorescence when it was added. To obtain the sequence information of the fragments to be tested, the sequencer captured the fluorescence signals and converted them into sequencing peaks through computer software. The DEGs were selected based on the following criteria: |log2 fold change| [?] 1 and $p< 0.05$. The pathway enrichment analysis of the DEGs was conducted by referring to the Kyoto Encyclopedia of Genes and Genomes (KEGG) database (Wang et al., 2017). The raw sequence data are available at NCBI

Sequence Read Archive (BioProject accession number: PRJNA877377).

2.5 Exogenous hormone and inhibitor treatment and enzyme activity assay

Sixty-day-old straight *P. yunnanensis* (S60) and twisty *P. yunnanensis* (T60) were sprayed with different concentrations of auxin (IAA), auxin inhibitors (Triiodobenzoic acid (TIBA) and auxinole), and*Pseudomonas syringae* . The assay was conducted in an artificial climate incubator (25 temperature, 16:8 h light:dark cycle, and 60% humidity). Graded levels of IAA (S18031, Yuanye, Shanghai) (0.1, 50, and 500 μm L^{-1}) (Zhao et al., 2019), TIBA (S30709, Yuanye, Shanghai) (50, 100, and 150 mg L^{-1}) (Zhang et al., 2017), and auxinole (HY-111444, MedChemExpress) (0.125, 0.25, and 0.5 mM) (Denbigh et al., 2020) working solutions were prepared by adding solute to distilled water and stirring the mixture until dissolution. The *P. syringae* slant, purchased from the Beijing Microbiological Culture Collection Center (Beijing, China), was placed in liquid medium and prepared into a bacterial solution with $OD_{600} = 0.1$. The controls of the hormone and *P. syringae* were distilled water and *P. syringae* medium, respectively. A randomized block design was employed in this assay with three replicates for each treatment. Each Yunnan pine plant was sprayed with 5 mL of the solution once a day for 55 days.

The treated plants were phenotyped and sampled to determine activities of acid invertase (BC0560, Solarbio, Beijing), phosphoenolpyruvate carboxylase (BC2190, Solarbio, Beijing), and phosphofructokinase (BC0530, Solarbio, Beijing); sucrose synthase synthesis direction (ml076692, Mlbio, Shanghai) and sucrose synthase decomposition direction (ml076680, Mlbio, Shanghai); and contents of cellulose (BC4280, Solarbio, Beijing), hemicellulose (BC4440, Solarbio, Beijing), and lignin (BC4200, Solarbio, Beijing) (Han et al., 2017).

2.6 Sucrose content assay

The content of sucrose was determined using HPLC (Cheng et al., 2018). Sucrose was extracted from Yunnan Pine by grounding, and it was then dissolved and filtered through a SEP-C18 cartridge (WAT021515; Waters, Shanghai, China) and Sep-Pak filter. A Waters 1525 HPLC system (Waters) was used to determine sucrose content. The column had an inner diameter of 6.5 mm × 300 mm and a particle size of 10 μm (Waters), with a guard column from Sugar-pak 1 Guard-Pak Holder and Insert (Waters). The column temperature was maintained at 85°C. The injection volume and flow rate of the mobile phase were 10 μl and 0.6 ml min^{-1}, respectively. Sucrose contents were determined according to an external standard solution. The concentration of each sample was calculated by the comparison of peak areas and retention times with those of calibrated sugar solutions of known concentrations (Lü et al., 2020). Three biological replicates were used for determining each index.

2.7 Validation of quantitative real-time PCR

Total RNA was isolated from the straight and twisty stem segments of Yunnan pines at three growth stages by using a plant RNA extraction kit (Tiangen, Beijing, China) (Xiao et al., 2020). In total, 19 DEGs were selected for quantitative real-time (qRT)-PCR analysis. The extracted RNA was reverse transcribed into cDNA by using the SuperScript III Platinum Two-Step qRT-PCR Kit (Invitrogen). qRT-PCR was performed following the protocol of TB Green Premix EX TaqTM II (Takara, Dalian, China) by using the 7300 Real-Time PCR System (Applied Biosystems, Carlsbad, USA). Actin was selected as an internal reference gene. Relative gene expression was quantified using the 2^{-Ct}method. Three biological replicates were used for each sample, and three technical replicates were used for each reaction. Corresponding primer sequences are presented in Table S1.

2.8 Immunohistochemistry

Tissue sections of stem segments of Yunnan pines were blocked for 1.5 h in blocking solution comprising 0.5% normal goat serum and 1% BSA. Primary antibodies (CDC2, AS06153; cFBPase, AS04043; PEPCK, AS07241; POR, AS05067; RbcL, AS03037A; SUS1, AS152830) were purchased from Agrisera and were diluted 1:500 in blocking solution. Following washing with PBS, the tissues were incubated in the primary antibody solution for 12–16 h at 4 and washed three times in PBS solution at room temperature (Nagaki & Yamaji, 2019). The secondary antibody was an anti-rabbit antibody from Abbkine (A21020). It was diluted

to 1:1000 in PBS and was added to the tissue sample, and then subjected to 2-h reactions at 37degC, washed three times with PBS, and developed using DAB.

2.9 Data processing

The DEG abundance patterns were analyzed using the standard procedure of the weighted gene co-expression network analysis (WGCNA) package in R (Langfelder & Horvath, 2008) and visualized using the pheatmap package. To interpret the biological functions of the DEGs identified, MapMan v. 3.6.0RC1 (Thimm et al., 2004) was used to display the data on biological process maps. For each assay, at least three biological replicates were used, with three independent technical replicates each, in addition to enzyme activity assays. To determine significant differences, one-way ANOVA was performed using the statistical program SPSS (version 13.0), followed by Duncan's multiple range test. Student's t -test and Pearson's correlation analysis were also conducted. Significance was accepted at the $p < 0.05$ level.

3 RESULTS

3.1 Inheritance of the twisty trait

In total, 120 plants in the F1 generation were produced by crossing twisty Yunnan pines with straight Yunnan pines. This cross produced 92 straight and 28 twisty Yunnan pines, approximately 3:1 ratio (Table 1), a chi-square test showed that the segregation fits a 3:1 ratio ($P>0.05$), indicating that the twisted trait was controlled by recessive alleles at a single locus.

3.2 Phenotypic indicator determination and tissue dissection of stem segments of Yunnan pines

To systematically compare the growth differences between straight and twisty Yunnan pines, plant height and DBH were used as indicators. The twisty type had a higher height gain than the straight type before 42 days after growth, whereas after 42 days, the former had a slower height gain and a slightly lower plant height than the latter (Figure 1). DBH of the straight type was larger than that of the twisty type at different growth stages.

In the natural environment, morphological differences between straight and twisty pines are easily discernible, as the twisty pines form a distinct twisty texture in the bark that is visible even after peeling (Figure 2A). To determine the main differences in histological anatomy between the straight and twisty stems of Yunnan pines, the stems at 30, 60, and 180 days were histologically sectioned and the tissue sections were stained with toluidine blue. The twisty pines at the same growth period showed more irregularly shaped xylem cells, significantly increased cell number, and more tightly arranged phloem cells compared with the straight pines. SEM revealed that the shape of xylem cells changed irregularly after trunk twisting. Moreover, the cells were more tightly arranged in the stem segments of 180-day-old twisty *P. yunnanensis* (T180) (Figure 2J, K). The longitudinal sections displayed that the xylem duct cells of the straight pines were smoother, whereas those of the twisty pines had significant breakage and stratification (Figure 2L, M). This indicated that stem twisting would affect ductal arrangement. Therefore, xylem and phloem were the main sites in which morphological differences occurred between straight and twisty Yunnan pines. Furthermore, we used LCM to enrich xylem and phloem materials from straight and twisty pines for downstream RNA-seq analysis.

3.3 Digital RNA-seq data and transcriptome assembly

The libraries of straight and twisty pines at three growth stages were sequenced to generate raw data. We used the Sanger quality score to evaluate data sequencing quality. The Phred mass fraction represents high-quality sequencing results obtained with values ranging from 97.13% to 98.32% for Q20 and 91.80% to 94.86% for Q30. All subsequent analyses were based on high-quality clean data. Because a reference genome was lacking, clean reads were assembled with Trinity software to obtain transcriptome sequence files. Short-read sequences were assembled into 77,931 unigenes (average length: 1194 bp); of them, 48,692 unigenes (62.48%) were 300–1000-bp long, 15,920 unigenes (20.43%) were 1000–2000-bp long, and 13,319 unigenes (17.09%) were >2000-bp long (Figure 3A). BUSCO (BenchUniversal Single-marking Copy Orthologs) was employed for the quality assessment of de novo assembled genes.

3.4 Functional annotation and classification

Different databases including NCBI non-redundant protein (Nr), NCBI non-redundant nucleotide sequence (Nt), UniProt/Swiss-Prot, Pfam, Kyoto Encyclopedia of Gene and Genomes (KEGG), KOG/COG, and Gene Ontology (GO) were used to annotate assembled unigenes. Numerous DEGs were identified at three growth stages: 30, 60, and 180 days. Of the total DEGs, 34 were mapped in all the three growth stages (Figure 3C). The KEGG enrichment analysis revealed that the DEGs were mainly involved in phytohormone signal transduction, photosynthetic carbon fixation, starch and sucrose metabolism, and plant–pathogen interaction pathways (Figure 3D, E). These results demonstrated that the twisted growth of the Yunnan pine stem is a complex biological process.

3.5 MapMan annotated metabolic pathways and WGCNA analysis

To comprehensively understand the biological metabolic processes of stem twisting in Yunnan pines, different algorithms were used to mine differential metabolic pathways. First, DEGs were enriched for the twisty vs straight type at different growth stages by using MapMan (Figures 4, S1, and S2). Compared with straight Yunnan pines, the twisty pines exhibited an increase and then a decrease in the expression of DEGs enriched in cell wall synthesis, lipid metabolism, sucrose metabolism, ascorbic acid cycle, and secondary metabolic pathways with an increase in growth time, in addition to a continuous decrease in the expression of light response-related DEGs. WGCNA was performed to analyze gene expression patterns in stem segments of Yunnan pines at different growth times, to cluster genes with similar expression patterns, and to analyze the correlation of each module with straight and twisty Yunnan pines at each developmental stage (Figure 5). Genes in the high-correlation modules that corresponded to different growth stages were enriched in the same metabolic pathways as those analyzed by KEGG and GO. This also confirmed the accuracy of the differential metabolic pathways screened in this study. Comparing the results of WGCNA, KEGG, and MapMan analyses, we selected the three pathways enriched in twisty pines at different growth stages for the study, namely starch and sucrose metabolism, photosynthetic carbon fixation, and phytohormone signal transduction.

3.6 DEGs involved in starch and sucrose metabolism

RNA-seq results showed that the expression of genes involved in carbohydrate hydrolysis pathways was low in twisty Yunnan pines. For instance, *INV* is involved in sucrose hydrolysis, *EXG* and*BGL* involved in glucose hydrolysis, and *CBH* involved in cellulose hydrolysis. The expression of starch and sucrose synthesis- related genes *BAM* and *Susy* was upregulated in twisty Yunnan pines (Figure 6).

3.7 DEGs involved in carbon fixation in photosynthetic organisms

In total, 23 DEGs related to the photosynthetic carbon fixation pathway were found (Figure 7). Of them, *PEPCK, AST, MDH,* and 14 genes of the *dmlA* family were involved in the C4 cycle. Overall, the expression levels of these genes were higher in straight Yunnan pines. Genes involved in the Calvin cycle, except *FBA* and*FBP* , were downregulated in twisty Yunnan pines. This suggested a great impact of trunk twisting on the pine's photosynthetic carbon fixation ability.

3.8 DEGs involved in plant hormone signal transduction

In total, 25 DEGs were upregulated in the phytohormone signaling pathway (Figure 8A), with most being enriched in auxin signal transduction pathways. In addition to *TIR1* , *ARF* and *SAUR* were downregulated in twisty Yunnan pines. Thus, we speculated that blocking auxin signal transduction leads to stem twisting. Further expression analysis of genes involved in the auxin metabolic pathway indicated that only *PIN* was upregulated in twisty pines (Figure 8B).

3.9 Spraying test of exogenous phytohormones and bacterial solution

Among the aforementioned three metabolic pathways, *ARF* ,*POR,* and *CBH* expressions were downregulated in twisty Yunnan pines, showing a co-expression trend. Therefore, a series of experiments was conducted to investigate the relationship between*ARF* , *POR,* and *CBH* expression and stem twisting. We conducted

spraying experiments of exogenous auxin IAA and auxin inhibitors. The experimental group was sprayed with the auxin signal transduction inhibitor auxinole as *ARF* is a critical gene of the auxin signal transduction pathway. The control group was sprayed with the same amount of distilled water as the experimental group. An exogenous auxin transport inhibitor, TIBA, was also sprayed to compare the responses of Yunnan pines to the two inhibitors. We found that plant–pathogen interaction metabolic pathways were more significantly enriched in straight Yunnan pines than in twisty Yunnan pines, in which three genes were associated with *P. syringae* . To test whether the plant–pathogen interaction ability changed after stem twisting, an experimental group sprayed with exogenous *P. syringae* bacterial solution was established. The exogenous auxin, auxin inhibitors, and bacterial suspension were sprayed onto the needles of 60-day-old Yunnan pines, followed by 50-day monitoring. Twisty Yunnan pines were more sensitive to IAA stimulation, as shown by the more pronounced increase in plant height of twisty pines after exogenous auxin addition compared with the control group (Figures 9A, B). TIBA and auxinole inhibited the plant height of straight pines more significantly. However, plants in the twisty group sprayed with auxinole stopped growing earlier than the straight plants (Figure 9 C–F). After spraying both straight and twisty pines with the bacterial solution for 55 days, the twisty pines grew significantly faster than the straight pines (Figure 9 G, H). This result was consistent with the KEGG enrichment results showing upregulated expression of plant–pathogen interacting genes in twisty Yunnan pines.

Biochemical characteristics of straight and twisty Yunnan pines sprayed with auxin and auxin inhibitors were examined. The enzyme activities of exogenous IAA-sprayed twisty Yunnan pines involved in sucrose metabolism (Figure 10A, D, E), photosynthetic carbon fixation (Figure 10B), and glycolysis (Figure 10C) pathways were significantly increased at each stage compared with the control group. TIBA had little effect on the twisty pines, but after exogenous auxinole treatment, both twisty and straight pines showed significantly decreased enzyme activities (Figure 10). Therefore, we concluded that stem twisting can enhance the disease resistance of Yunnan pines, which may result from its long-term adaptability. However, inhibition of auxin signal transduction may seriously affect the normal growth of Yunnan pines.

3.10 Immunohistochemistry

To further identify the metabolic pathways involved in twisty and straight traits at the protein level, we immunolocalized antibodies corresponding to *POR* , *RbcL* , *Susy* , *FBP* ,*PEPCK,* and *CDC2* in the sections of stem segments of straight and twisty pines that were 30-, 60-, and 180-day old (Figure 11). The six proteins were specifically detected in the stems of both straight and twisty pines. The expression signals of CDC2 involved in cell division, cFBPase and PEPCK involved in gluconeogenesis, and SUS1 involved in sucrose metabolism were stronger in the 30-day-old straight*P. yunnanensis* (S30) than in the 30-day-old twisty *P. yunnanensis* (T30). The SUS1 and PEPCK expression signals were stronger in T60 than in S60. POR and RbcL are closely related to photosynthesis. Because the stem is not the main photosynthetic organ, POR and RbcL expression signals were weak in the stem segments and weaker in the twisty stem segments. Expression signals of these six proteins were stronger in the straight pines than in the twisty pines by 180 days of growth. Accordingly, we speculated that twisted stem growth would decrease the expression of crucial proteins required for the growth and development of Yunnan pines and adversely affect their development.

3.11 Comparison of cellulose, hemicellulose, and lignin contents in stem segments of straight and twisty Yunnan pines

CBH is a key gene regulating cellulolytic processes and is downregulated in all growth stages of Yunnan pines. We, therefore, determined cellulose, hemicellulose, and lignin contents in the stem segments of S60, S180, T60, and T180. The cellulose content was significantly higher in twisty pines than in straight pines (Figure 12A). This indicated that *CBH* expression downregulation did hinder cellulolysis in twisty Yunnan pines, allowing cellulose accumulation in the twisty plant. The lignin content was significantly lower in the twisty Yunnan pines than in the straight Yunnan pines (Figure 12B); the hemicellulose content did not reflect a close correlation between the two groups (Figure 12C). The sucrose content was significantly higher in twisty pines than in straight pines (Figure 12D).

3.12 Validation by qRT-PCR

To further validate the reliability of the RNA-seq analysis data, 19 DEGs were validated using qRT-PCR (Figure 13). These DEGs were associated with cell division (*CDC2*), starch and sucrose metabolism (*BAM* , *BGL* , *CBH* , *cFBPase* ,*INV* , *PEPCK* , and *SUS1*), photosynthesis (*FBA* ,*FBP* , *PGK* , *POR* , *RbcL* , and *XFP*), and phytohormone synthesis and signal transduction (*ARF* , *SAUR* ,*TIR1* , *PIN* , and *YUC*). The qRT-PCR results were generally consistent with the RNA-seq analysis results, confirming the accuracy of the RNA-seq results. According to the results, the expressions of *ARF* , *POR,* and *CBH* were downregulated in twisty Yunnan pines, showing a co-expression trend.

4 DISCUSSION

4.1 Inheritance of trunk twisting

To investigate whether trunk twisting in *P. yunnanensis* is caused by environmental or genetic factors, He et al. (1994) speculated that twisty and straight trunks are a pair of relative traits controlled by a pair of alleles; of them, twisty trunk is dominant and straight trunk is recessive, as determined through progeny tests. Using molecular marker assays, Xu et al. (2015) reported that the straight pine and twisty pine populations exhibit no significant genetic differences, supporting the belief that twisty pines are an ecological type of Yunnan pines. In this study, crossing twisty pines with straight pines resulted in a seedling ratio of 92 straight: 28 twisty, consistent with the segregation ratio of 3:1. This suggested that recessive genes control the trait of twisted growth in Yunnan pines. This result is similar to that of Smith et al.'s study (Smith & Mehlenbacher, 1996) on twisted *C. avellana* . Smith et al. conducted a 6-year hybrid experiment on different varieties of*C. avellana* from 1987. Crossing of twisty *C. avellana* with each normal variety produced no twisted progenies. However, self-crossing of twisty *C. avellana* with another twisty *C. avellana* resulted in 3 normal: 1 twisted progeny. To identify trunk twisting as a stable inherited trait, the resulting twisty progenies were backcrossed with the twisty plants, and a segregation ratio of 1 normal: 1 twisty was obtained. Yoshida (1994) statistically analyzed segregation patterns in self-pollinated and crossed progenies of two lines of *Trifolium pratense* (*Poncirus trifoliate*). The study found that the two dwarf *Trifolium* varieties were controlled by one and two recessive genes, respectively. Recessive genes also control the left-handed helix of tomato stems (Yang et al., 2020). However, Lin et al. (2007) studies the phenotypic statistics of the progenies obtained from a cross of twisty *Salix matsudana* with wild-type plants and concluded that the twisty phenotype is controlled by a dominant gene. Identification of recessive genes as the controller for trunk twisting of Yunnan pines provides guidance for future breeding of this plant. Accordingly, artificial emasculation or pollination of Yunnan pines can be performed to ensure stable inheritance of the straight trunk trait and to provide richer germplasm resources for its breeding.

4.2 RNA-seq based on LCM

Xylem and phloem cells were collected from frozen sections of straight and twisty stem segments at different growth stages by using LCM. RNA was extracted from the collected cells, linearly amplified, and transcriptome-sequenced using RNA-seq. Consequently, 2,386 DEGs significantly associated with trunk twisting were obtained. The combination of LCM with RNA-seq has been widely used in woody plant research. For example, Turner et al. (2018) enriched epithelial cells of resin secretory ducts in *P. taeda* needles by using LCM and compared them with the genes expressed in mesophyll cells. They reported that 487 genes involved in resin biosynthesis were significantly enriched in the epithelial cells. Difficult regulation of adventitious root development is a major obstacle to the reproduction of woody plants of commercial value. To regulate adventitious root development from a molecular viewpoint, Stevens et al. (2018) enriched cortical, phloem fiber, or phloem parenchyma cells in the stem segments of *Juglans nigra* L. by using LCM and performed RNA-seq. After qRT-PCR analysis, mRNA abundance of nine root-related genes was found to be changed. Ranjan et al. (2022) enriched cambium cells from the stem cuttings of two hybrid poplar cultivars (easy and difficult rooting cultivars). They identified 17,997 genes significantly associated with adventitious root formation through RNA-seq. Major regulators of adventitious root development were successfully mapped by combining LCM with RNA-seq. Radiation cells can play a role in tracheid lignification.

To test this hypothesis, radiation cells and tracheids from tangential cryosections of *P. abies* xylem were enriched with LCM, and 1,073 DEGs were detected using RNA-seq (Blokhina et al., 2019). A gene expressed only in radiation cells was identified, and the results exhibited that the genes related to the biosynthesis pathway of lignin monomers were active in radiation cells. This finding suggested that radiation cells could produce monomers that contribute to lignification of tracheid cell walls. LCM combined with RNA-seq provides single-copy genes as molecular markers for seed plant phylogeny (Li et al., 2017). The LCM and RNA-seq technology combination greatly improves the research efficiency and accuracy. This combination realizes more targeted research on the research object and focuses on the sites where differences occur.

4.3 Twisting phenomenon alters metabolic pathways

RNA-seq analysis of LCM-enriched materials revealed *POR* ,*CBH* , and *ARF* co-expression. Moreover, KEGG enrichment, WGCNA, and MapMan analyses combined with physiological and biochemical parameter assessment revealed that the cellulose content increased and the lignin content decreased in twisty Yunnan pines compared with those in straight pines. When stimulated by gravity, stems and branches of woody plants form tension wood, which is usually the inclined or bent upper side of the trunk or branch, that is, the xylem of the tensioned site. The characteristic of tension wood differing from that of ordinary wood is mainly the fibers formed with gelatinous cell wall layers composed of crystalline cellulose (Andersson-Gunnera et al., 2006). Therefore, the content of cellulose is high in tension wood, and it lacks lignin and hemicellulose. The xylem material from stem segments in poplar tension wood formed at an early stage was subjected to transcriptome analysis. This analysis revealed significant enrichment of genes involved in gibberellin and brassinolide pathways, as well as flavonoid and phosphoinositide pathways (Collings et al., 2021). The results indicated that these pathways may have a role in twisting morphogenesis. RNA-seq of tension wood formed in California poplar revealed that the genes related to lignin and cellulose biosynthesis were downregulated and upregulated, respectively, in tension wood (Kerwin, 2021). This result was also obtained in tension wood formed by *P. trichocarpa* and*Betula luminifera* (Cai et al., 2018; Liu et al., 2021). In addition, studies on gerbera (Hamedan et al., 2019), maize (Sun et al., 2018), and soybean (Hussain et al., 2021) have shown that an increase in the content of lignin, a secondary cell wall component, negatively affects the stem strength and reduces stem bending or lodging. Because the expression of the cellulolytic gene *CBH* was downregulated in twisty Yunnan pines, we determined the cellulose and lignin contents in stem segments of S60, S180, T60, and T180. We found that the cellulose content in twisty pines was significantly increased, similar to that in tension wood. By contrast, the lignin content decreased, thereby reducing the stem hardness of Yunnan pines and creating conditions for the twisted growth.

Genes involved in cellulose synthesis, lignification, cytoskeletal development, signaling, and stress response were identified in poplar tension wood (Azri et al., 2013). Tension wood formation-induced alterations in cell wall traits result from a combination of lignin biosynthesis downregulation and hemicellulose remodeling rather than the frequently proposed notion of the activation of cellulose biosynthesis pathways (Mizrachi et al., 2014). When auxin signal transduction is compromised, cellulose biosynthesis is promoted, thereby accelerating tension wood formation. Therefore, increase expression of auxin transport-related genes is considered the most important cause of twisted growth (Yu et al., 2016). Verger et al. (2019) found that*Arabidopsis* organs also exhibit twisted growth when auxin correspondence or transport is affected. Felten et al. (2018) and Seyfferth et al. (2019) found that ethylene also induces tension wood formation.

A regulatory relationship does exist between auxin and cellulose (Lehman & Sanguinet, 2019). Xin et al. (2020) concluded that auxin alters the interaction between cellulose microfibrils in the cell wall because cell wall elongation depends on cell wall acidification and auxin plays a vital role in acid growth. Ehrhardt et al. suggested that auxin controls cellulose deposition in the cell wall by regulating cortical microtubule arrangement (Echevin et al., 2019, Ehrhardt & Shaw, 2006). Wang et al. (2020) successfully mapped auxin-related genes that affect the cellulose content in plants. These genes include the auxin signal transduction gene *SAUR* , which stimulates apoplast acidification and cell wall loosening, and the auxin transport gene *PIN* , whose polar localization is limited by cellulose deposition. Therefore, cellulose deposition is believed to affect auxin distribution in plant species. Fruit softening involves cellulose hydrolysis in the cell wall, and

Qian et al. (2022) identified the auxin-related genes *ARF* ,*SAUR,* and *TIR1* involved in fruit softening. Studies have revealed an indirect regulatory relationship between auxin and cellulose, and auxin-related genes can affect photosynthesis. Yuan et al. (2018) found that *S1ARF10,* a member of the ARF family of tomato, positively regulates *POR* to affect chlorophyll metabolism. This increases the starch, fructose, and sucrose contents in tomatoes. Liu et al. (2021) performed a transcriptomic analysis of transgenic *A. thaliana* overexpressing the right-handed helical gene *SmSPR1* and discovered that numerous DEGs were involved in plant light signal reception, chlorophyll synthesis, and photosystem building. Moreover, they found that the genes involved in light signal transduction were co-expressed with auxin-related genes, indicating that the light response and auxin signaling pathways may have crucial roles in etiolated spiral growth.

The auxin signal transduction gene *ARF* , chlorophyll synthesis gene *POR* , and cellulolytic gene *CBH* in twisty Yunnan pines were also mapped in this study. Based on the results of control experiments with the addition of exogenous auxin and auxin inhibitors, immunohistochemical techniques, and physiological index determination, we introduced a working model for the molecular mechanism underlying trunk twisting in Yunnan pines (Figure 14). Downregulation of *ARF*expression blocks auxin signal transduction in Yunnan pines in an unfavorable growth environment. This leads to the downregulation of*POR* expression, thereby impeding chlorophyll synthesis and hindering the normal photosynthesis. In addition, *ARF* can upregulate *Susy* expression and increase the sucrose content (Figure 11, Figure 12D, Figure 13), which allows a large amount of sucrose to synthesize cellulose. However, due to downregulated*CBH* expression and abnormal cellulolysis, cellulose accumulates and the lignin content decreases in Yunnan pines, eventually making the stem highly prone to twisted growth. However, the exact molecular mechanism of how auxin-related genes regulate chlorophyll synthesis and cellulose breakdown has not been elucidated, warranting further research.

5 CONCLUSION

The present study explained the molecular differences between twisty and straight Yunnan pines and provided theoretical references for its breeding. Through a diallel cross experiment, we found that recessive genes control the heritable trait of trunk twisting in Yunnan pines. Tissue dissection was performed to identify the sites that resulted in the differences between twisty and straight pines. LCM was used to enrich materials from the sites for RNA-seq analysis. A combination of RNA-seq analysis and metabolic pathways enriched by WGCNA and MapMan successfully mapped three genes co-expressed in twisty Yunnan pines, namely *ARF* , *POR,* and *CBH* . Furthermore, the model of trunk twisting formation in Yunnan pines was established by applying exogenous hormones and inhibitors and through immunohistochemical techniques and physiological index determination. Auxin signal transduction is inhibited and auxin synthesis and transport are affected in Yunnan pines in an unfavorable growth environment. With the downregulation of the key gene (*POR*) for chlorophyll synthesis, chlorophyll synthesis is blocked and photosynthesis is weakened. Under-expression of the gene *CBH* , which is involved in cellulolysis, leads to cellulose accumulation and a decrease in the lignin content in twisty pines. This reduces the stem hardness, making the stem more prone to twisting. Because *ARF* can directly and indirectly regulate *POR* and *CBH* , *ARF* expression may be used as an accurate and convenient indicator for trunk shape evaluation in Yunnan pines.

ACKNOWLEDGEMENTS

This work was funded by the Essential Scientific Research of Chinese National Nonprofit Institute (CAFYBB2019ZB006 and CAFYBB2021ZW003), Yunnan Applied Basic Research Projects (2019FA013), National Natural Science Foundation of China (32022058), and Training Objects of Technological Innovation Talents in Yunnan Province (2019HB074). The authors declare that they have no conflict of interest.

CONFLICT OF INTEREST

The authors declare no conflict of interest.

REFERENCES

Abbott, E., Hall, D., Hamberger, B., & Bohlmann, J. (2010). Laser microdissection of conifer stem tissues: Isolation and analysis of high quality RNA, terpene synthase enzyme activity and terpenoid metabolites

from resin ducts and cambial zone tissue of white spruce (*Picea glauca*). *BMC Plant Biology, 10* (1), 106.*https://doi.org/10.1186/1471-2229-10-106*.

Abe, M., Yoshikawa, T., Nosaka, M., Sakakibara, H., Sato, Y., Nagato, Y., & Itoh, J.-i. (2010). *WAVY LEAF1* , an ortholog of Arabidopsis*HEN1* , regulates shoot development by maintaining MicroRNA and trans-acting small interfering RNA accumulation in rice. *PLANT PHYSIOLOGY, 154* (3), 1335-1346.*https://doi.org/10.1104/pp.110.160234*.

Agusti, J., Lichtenberger, R., Schwarz, M., Nehlin, L., & Greb, T. (2011). Characterization of transcriptome remodeling during cambium formation identifies *MOL1* and *RUL1* as opposing regulators of secondary growth. *PLoS Genet, 7* (2), e1001312.*https://doi.org/10.1371/journal.pgen.1001312*.

Andersson-Gunnera, S., Mellerowicz, E. J., Love, J., Segerman, B., Ohmiya, Y., Coutinho, P. M., Nilsson, P., Henrissat, B., Moritz, T., & Sundberg, B. (2006). Biosynthesis of cellulose-enriched tension wood in Populus: global analysis of transcripts and metabolites identifies biochemical and developmental regulators in secondary wall biosynthesis.*The Plant Journal, 45* (2), 144-165.*https://doi.org/10.1111/j.1365-313X.2005.02584.x*.

Azri, W., Ennajah, A., Nasr, Z., Woo, S.-Y., & Khaldi, A. (2013). Transcriptome profiling the basal region of poplar stems during the early gravitropic response. *Biologia Plantarum, 58* , 55-63.*https://doi.org/10.1007/s10535-013-0364-7*.

Blokhina, O., Laitinen, T., Hatakeyama, Y., Delhomme, N., Paasela, T., Zhao, L., Nathaniel R., S., Hiroshi, W., Anna, K., & Fagerstedt, K. (2019). Ray Parenchymal Cells Contribute to Lignification of Tracheids in Developing Xylem of Norway Spruce. *Plant Physiology, 181* (4), 1552-1572.*https://doi.org/10.1104/pp.19.00743*.

Blokhina, O., Valerio, C., Sokołowska, K., Zhao, L., Kärkönen, A., Niittylä, T., & Fagerstedt, K. (2016). Laser Capture Microdissection Protocol for Xylem Tissues of Woody Plants. *Frontiers in Plant Science, 07* (106), 01965.*https://doi.org/10.3389/fpls.2016.01965*.

Bringmann, M., Li, E., Sampathkumar, A., Kocabek, T., Hauser, M.-T., & Persson, S. (2012). POM-POM2/Cellulose synthase Interacting1 Is Essential for the Functional Association of Cellulose Synthase and Microtubules in Arabidopsis. *The Plant Cell, 24* (1), 163-177.*https://doi.org/10.1105/tpc.111.093575*.

Burgess, A. J., Gibbs, J. A., & Murchie, E. H. (2019). A canopy conundrum: can wind-induced movement help to increase crop productivity by relieving photosynthetic limitations? *Journal of Experimental Botany, 70* (9), 2371-2380.*https://doi.org/10.1093/jxb/ery424*.

Cai, M., Huang, H., Ni, F., Tong, Z., Lin, E., & Zhu, M. (2018). RNA-Seq analysis of differential gene expression in *Betula luminifera* xylem during the early stages of tension wood formation.*PeerJ, 6* (8), e5427.*https://doi.org/10.7717/peerj.5427*.

Cañas, R. A., Canales, J., Gómez-Maldonado, J., Ávila, C., & Cánovas, F. M. (2014). Transcriptome analysis in maritime pine using laser capture microdissection and 454 pyrosequencing. *Tree Physiology, 34* (11), 1278-1288.*https://doi.org/10.1093/treephys/tpt113*.

Chakraborty, J., Luo, J., & Dyson, R. J. (2021). Lockhart with a twist: Modelling cellulose microfibril deposition and reorientation reveals twisting plant cell growth mechanisms. *Journal of Theoretical Biology, 525* , 110736.*https://doi.org/10.1016/j.jtbi.2021.110736*.

Chen, Y., Bai, Q., Ruan, F., & Su, S. (2019). Proteomic analysis of differently expressed proteins in sex differentiation phases of flower buds in monoecious *Pistacia chinensis* Bunge. *Israel Journal of Plant Sciences, 66* (3-4), 1-14.*https://doi.org/10.1163/22238980-20191063*.

Cheng, R., Cheng, Y., Lü, J., Chen, J., Wang, Y., Zhang, S., & Zhang, H. (2018). The gene *PbTMT4* from pear (*Pyrus bretschneideri*) mediates vacuolar sugar transport and strongly affects sugar accumulation in fruit. *Physiologia Plantarum, 164* (3), 307-319.*https://doi.org/10.1111/ppl.12742*.

Collings, D. A., Thomas, J., Dijkstra, S. M., & Harrington, J. J. (2021). The formation of interlocked grain in African mahogany (*Khaya* spp.) analysed by X-ray computed microtomography. *Tree Physiology, 41* (8), 1542-1557.*https://doi.org/10.1093/treephys/tpab020*.

Day, R. C., Grossniklaus, U., & Macknight, R. C. (2005). Be more specific! Laser-assisted microdissection of plant cells. *Trends in Plant Science, 10* (8), 397-406.*https://doi.org/10.1016/j.tplants.2005.06.006*.

Denbigh, G. L., Dauphinee, A. N., Fraser, M. S., Lacroix, C. R., & Gunawardena, A. H. L. A. N. (2020). The role of auxin in developmentally regulated programmed cell death in lace plant. *American Journal of Botany, 107* (4), 577-586.*https://doi.org/10.1002/ajb2.1463*.

Echevin, E., Gloanec, C. L., Skowrońska, N., Routier-Kierzkowska, A.-L., Burian, A., & Kierzkowski, D. (2019). Growth and biomechanics of shoot organs. *Journal of Experimental Botany, 70* (14), 3573-3585.*https://doi.org/10.1093/jxb/erz205*.

Ehrhardt, D. W., & Shaw, S. L. (2006). Microtubule dynamics and organization in the plant cortical array. *Annual review of plant biology, 57* , 859-875.*https://doi.org/10.1146/annurev.arplant.57.032905.105329*.

Emonet, A., & Hay, A. (2022). Development and diversity of lignin patterns. *PLANT PHYSIOLOGY, 0* (0), 1-13.*https://doi.org/10.1093/plphys/kiac261*.

Falandysz, J., Wang, Y., & Saniewski, M. (2021). 137Cs and 40K activities and total K distribution in the sclerotia of the Wolfiporia cocos fungus from China. *Journal of Environmental Radioactivity, 231* (2), 106549.*https://doi.org/10.1016/j.jenvrad.2021.106549*.

Fan, Y., Zhang, S., ZengquanLan, & Lan, Q. (2021). Possible causes for the differentiation of *Pinus yunnanensis* and *P. Kesiya*var. Langbianensis in Yunnan, China: Evidence from seed germination. *Forest Ecology and Management, 494* (2), 119321.*https://doi.org/10.1016/j.foreco.2021.119321*.

Felten, J., Vahala, J., Love, J., Gorzsás, A., Rüggeberg, M., Delhomme, N., Leśniewska, J., Kangasjärvi, J., Hvidsten, T. R., Mellerowicz, E. J., & Sundberg, B. (2018). Ethylene signaling induces gelatinous layers with typical features of tension wood in hybrid aspen. *New Phytologist, 218* (3), 999-1014.*https://doi.org/10.1111/nph.15078*.

Goué, N., Noël-Boizot, N., Vallance, M., Magel, E., & Label, P. (2012). Microdissection to Isolate Vascular Cambium Cells in Poplar. *Silva Fennica, 46* (1), 5-16.*https://doi.org/10.14214/sf.62*.

Guo, K., Huang, C., Miao, Y., Cosgrove, D. J., & Hsia, K. J. (2022). Leaf morphogenesis: The multifaceted roles of mechanics. *Molecular Plant, 15* (7), 1098-1119.*https://doi.org/10.1016/j.molp.2022.05.015*.

Hamedan, H. J., Sohani, M. M., Aalami, A., & Nazarideljou, M. J. (2019). Genetic engineering of lignin biosynthesis pathway improved stem bending disorder in cut gerbera (*Gerbera jamesonii*) flowers. *Scientia Horticulturae, 245* , 274-279.*https://doi.org/10.1016/j.scienta.2018.10.013*.

Han, X., He, X., Qiu, W., Lu, Z., Zhang, Y., Chen, S., Liu, M., Qiao, G., & Zhuo, R. (2017). Pathogenesis-related protein PR10 from *Salix matsudana* Koidz exhibits resistance to salt stress in transgenic *Arabidopsis thaliana* . *Environmental and Experimental Botany, 141* , 74-82.*https://doi.org/10.1016/j.envexpbot.2017.07.008*.

Hao, S., Su, W., & Li, Q. Q. (2021). Adaptive roots of mangrove *Avicennia marina* : Structure and gene expressions analyses of pneumatophores. *Science of The Total Environment, 757* (3), 143994.*https://doi.org/10.1016/j.scitotenv.2020.143994*.

He, F. 1994. Genetic test of offspring of Yunnan pine wood texture phenotypic traits. *Western Forestry Science,* 2**,** 1-7.

Hussain, S., Shuxian, L., Mumtaz, M., Shafiq, I., Iqbal, N., Brestic, M., Shoaib, M., Sisi, Q., Li, W., Mei, X., Bing, C., Zivcak, M., Rastogi, A., Skalicky, M., Hejnak, V., Weiguo, L., & Wenyu, Y. (2021).

Foliar application of silicon improves stem strength under low light stress by regulating lignin biosynthesis genes in soybean (*Glycine max* (L.) Merr.). *Journal of Hazardous Materials, 401* , 123256.*https://doi.org/10.1016/j.jhazmat.2020.123256*.

Kerwin, R. E. (2021). Under pressure: transcriptional regulation of tension wood in *Populus trichocarpa* (California poplar).*PLANT PHYSIOLOGY, 186* (1), 212-214.*https://doi.org/10.1093/plphys/kiab096*.

Langer, M., Hegge, E., Speck, T., & Speck, O. (2021). Acclimation to wind loads and/or contact stimuli? A biomechanical study of peltate leaves of *Pilea peperomioides* . *Journal of Experimental Botany, 73* (4), 1236-1252.*https://doi.org/10.1093/jxb/erab541*.

Langfelder, P., & Horvath, S. (2008). WGCNA: an R package for weighted correlation network analysis. *BMC Bioinformatics, 9* , 559.*https://doi.org/10.1186/1471-2105-9-559*.

Lehman, T. A., & Sanguinet, K. A. (2019). Auxin and Cell Wall Crosstalk as Revealed by the *Arabidopsis thaliana* Cellulose Synthase Mutant*Radially Swollen 1* . *Plant & Cell Physiology, 60* (7), 1487-1503.*https://doi.org/10.1093/pcp/pcz055*.

Li, S., Lei, L., Somerville, C. r., & Gu, Y. (2012). Cellulose synthase interactive protein 1 (CSI1) links microtubules and cellulose synthase complexes. *Proceedings of the National Academy of Sciences of the United States of America, 109* (1), 185-190.*https://doi.org/10.1073/pnas.1118560109*.

Li, Y., Li, M., Ming, A., Wang, H., Yu, S., & Ye, S. (2021). Spatial pattern dynamics among co-dominant populations in early secondary forests in Southwest China. *Journal of Forestry Research, 32* (4), 1373-1384.*https://doi.org/10.1007/s11676-020-01207-6*.

Li, Z., Torre, A. R. D. L., Sterck, L., Cánovas, F. M., Avila, C., Merino, I., Cabezas, J. A., Cervera, M. T., Ingvarsson, P. K., & Peer, Y. V. d. (2017). Single-Copy Genes as Molecular Markers for Phylogenomic Studies in Seed Plants. *Genome Biology and Evolution, 9* (5), 1130-1147.*https://doi.org/10.1093/gbe/evx070*.

Lin, J., Gunter, L., Harding, S., Kopp, R. F., McCord, R. P., Tsai, C.-J., Tuskan, G. A., & Smart, L. B. (2007). Development of AFLP and RAPD markers linked to a locus associated with twisted growth in corkscrew willow (*Salix matsudana* 'Tortuosa'). *Tree Physiology, 27* (11), 1575-1583.*https://doi.org/10.1093/treephys/27.11.1575*.

Liu, B., Liu, J., Yu, J., Wang, Z., Sun, Y., Li, S., Lin, Y. C. J., Chiang, V. L., Li, W., & Wang, J. P. (2021). Transcriptional reprogramming of xylem cell wall biosynthesis in tension wood.*PLANT PHYSIOLOGY, 186* (1), 250-269.*https://doi.org/10.1093/plphys/kiab038*.

Liu, X., Zhang, J., Xue, L., & Rao, G. (2021). Transcriptome-wide effect of *Salix SmSPR1* in etiolated seedling of*Arabidopsis* . *Journal of Forestry Research, 32* (3), 975-985.*https://doi.org/10.1007/s11676-020-01202-x*.

Liu, Y., Xu, F., Gou, J., Al-Haddad, J., Telewski, F. W., Bae, H.-J., & Joshi, C. P. (2012). Importance of two consecutive methionines at the N-terminus of a cellulose synthase (PtdCesA8A) for normal wood cellulose synthesis in aspen. *Tree Physiology, 32* (11), 1403-1412.*https://doi.org/10.1093/treephys/tps096*.

Lopez, D., Franchel, J., Venisse, J.-S., Drevet, J. R., Label, P., Coutand, C., & Roeckel-Drevet, P. (2021). Early transcriptional response to gravistimulation in poplar without phototropic confounding factors. *AoB PLANTS, 13* (1), plaa071.*https://doi.org/10.1093/aobpla/plaa071*.

Lü, J., Tao, X., Yao, G., Zhang, S., & Zhang, H. (2020). Transcriptome Analysis of Low- and High-Sucrose Pear Cultivars Identifies Key Regulators of Sucrose Biosynthesis in Fruits. *Plant and Cell Physiology, 61* (8), 1493-1506.*http://doi.org/10.1093/pcp/pcaa068*.

Mizrachi, E., Maloney, V. J., Silberbauer, J., Hefer, C. A., Berger, D. K., Mansfield, S. D., & Myburg, A. A. (2014). Investigating the molecular underpinnings underlying morphology and changes in

carbon partitioning during tension wood formation in *Eucalyptus* .*New Phytologist, 206* (4), 1351-1363.*https://doi.org/10.1111/nph.13152*.

Nagaki, K., & Yamaji, N. (2019). Decrosslinking enables visualization of RNA-guided endonuclease–*in situ* labeling signals for DNA sequences in plant tissues. *Journal of Experimental Botany, 71* (6), 1792-1800.*https://doi.org/10.1093/jxb/erz534*.

Nagy, N. E., Sikora, K., Krokene, P., Hietala, A. M., Solheim, H., & Fossdal, C. G. (2014). Using laser micro-dissection and qRT-PCR to analyze cell type-specific gene expression in Norway spruce phloem.*PeerJ, 29* (2), e362.*https://doi.org/10.7717/peerj.362*.

Olsen, S., & Krause, K. (2019). A rapid preparation procedure for laser microdissection-mediated harvest of plant tissues for gene expression analysis. *Plant Methods, 15* (1), 88.*https://doi.org/10.1186/s13007-019-0471-3*.

Pan, Y., Chen, P., Lu, J., Zhou, X. D., & Ye, H. (2017). First report of blue-stain in *Pinus yunnanensis* caused by ophiostoma tingens associated with tomicus minor in China. *Journal of Plant Pathology, 99* (3), 799-818.*http://dx.doi.org/10.4454/jpp.v99i3.3931*.

Polko, J. K., & Kieber, J. J. (2019). The Regulation of Cellulose Biosynthesis in Plants. *The Plant Cell, 31* (2), 282-296.*https://doi.org/10.1105/tpc.18.00760*.

Qian, J., Zhao, Y., Shi, Y., & Chen, K. (2022). Transcriptome analysis of peach fruit under 1-MCP treatment provides insights into regulation network in melting peach softening. *Food Quality and Safety .https://doi.org/10.1093/fqsafe/fyac048*.

Ram, H., Singh, A., Katoch, M., Kaur, R., Sardar, S., Palia, S., Satyam, R., Sonah, H., Deshmukh, R., Pandey, A. K., Gupta, I., & Sharma, T. R. (2020). Dissecting the nutrient partitioning mechanism in rice grain using spatially resolved gene expression profiling. *Journal of Experimental Botany, 72* (6), 2212-2230.*https://doi.org/10.1093/jxb/eraa536*.

Ranjan, A., Perrone, I., Alallaq, S., Singh, R., Rigal, A., Brunoni, F., Chitarra, W., Guinet, F., Kohler, A., Martin, F., Street, N. R., Bhalerao, R., Legué, V., & Bellini, C. (2022). Molecular basis of differential adventitious rooting competence in poplar genotypes.*Journal of Experimental Botany, 73* (12), 4046-4064.*https://doi.org/10.1093/jxb/erac126*.

Seyfferth, C., Wessels, B. A., Gorzsás, A., Jonathan W. Love3, Rüggeberg, M., Delhomme, N., Vain, T., Antos, K., Tuominen, H., Sundberg, B., & Felten, J. (2019). Ethylene signaling is required for fully functional tension wood in hybrid Aspen. *Frontiers in Plant Science, 10* , 1101.*https://doi.org/10.3389/fpls.2019.01101*.

Shavnin, S. A., Ovchinnikov, I. S., Golikov, D. Y., Montile, A. A., Galako, V. A., & Vlasenko, V. E. (2018). Phenomenon of Trunk Twist during the Growth of Woody Plants (Using the Example of *Pinus sylvestris* L. and *Picea obovata* Ldb.). *Contemporary Problems of Ecology, 11* (1), 72-78.*https://doi.org/10.1134/S1995425518010122*.

Shinozaki, Y., Nicolas, P., Fernandez-Pozo, N., Ma, Q., Evanich, D. J., Shi, Y., Xu, Y., Zheng, Y., Snyder, S. I., Martin, L.B. B., Ruiz-May, E., Thannhauser, T. W., Chen, K., Domozych, D. S., Catalá, C., Fei, Z., Mueller, L. A., Giovannoni, J. J., & Rose, J. K. C. (2018). High-resolution spatiotemporal transcriptome mapping of tomato fruit development and ripening. *Nature Communications, 9* (1), 364.*https://doi.org/10.1038/s41467-017-02782-9*.

Smith, D. C., & Mehlenbacher, S. A. (1996). Inheritance of contorted growth in hazelnut. *Euphytica, 89* (2), 211-213.*https://doi.org/10.1007/BF00034607*.

Stevens, M. E., Woeste, K. E., & Pijut, P. M. (2018). Localized gene expression changes during adventitious root formation in black walnut (*Juglans nigra* L.). *Tree Physiology, 38* (6), 877-894.*https://doi.org/10.1093/treephys/tpx175*.

Sun, Q., Liu, X., Yang, J., Liu, W., Du, Q., Wang, H., Fu, C., & Li, W. (2018). MicroRNA528 Affects Lodging Resistance of Maize by Regulating Lignin Biosynthesis under Nitrogen-Luxury Conditions. *Molecular Plant, 11* (6), 806-814.*https://doi.org/10.1016/j.molp.2018.03.013*.

Takahashi, H., Kamakura, H., Sato, Y., Shiono, K., Abiko, T., Tsutsumi, N., Nagamura, Y., Nishizawa, N. K., & Nakazono, M. (2010). A method for obtaining high quality RNA from paraffin sections of plant tissues by laser microdissection. *Journal of Plant Research, 123* (6), 807-813.*https://doi.org/10.1007/s10265-010-0319-4*.

Tao, G., Ramakrishnan, M., Vinod, K. K., Yrjälä, K., Satheesh, V., Cho, J., Fu, Y., & Zhou, M. (2020). Multi-omics analysis of cellular pathways involved in different rapid growth stages of moso bamboo. *Tree Physiology, 40* (11), 1487-1508.*https://doi.org/10.1093/treephys/tpaa090*.

Thimm, O., Blasing, O., Gibon, Y., Nagel, A., Meyer, S., Kruger, P., Selbig, J., Muller, L. A., Rhee, S. Y., & Stitt, M. (2004). MAPMAN: a user-driven tool to display genomics data sets onto diagrams of metabolic pathways and other biological processes. *The Plant Journal, 37* (6), 914-939.*https://doi.org/10.1111/j.1365-313x.2004.02016.x*.

Thitamadee, S., Tuchihara, K., & Hashimoto, T. (2002). Microtubule basis for left-handed helical growth in Arabidopsis. *Nature, 417* (6885), 193-196.*https://doi.org/10.1038/417193a*.

Turner, G. W., Parrish, A. N., Zager, J. J., Fischedick, J. T., & Lange, B. M. (2018). Assessment of flux through oleoresin biosynthesis in epithelial cells of loblolly pine resin ducts. *Journal of Experimental Botany, 70* (1), 217-230.*https://doi.org/10.1093/jxb/ery338*.

Verger, S., Liu, M., & Hamant, O. (2019). Mechanical Conflicts in Twisting Growth Revealed by Cell-Cell Adhesion Defects. *Frontiers in Plant Science, 10* (173), 1-9.*https://doi.org/10.3389/fpls.2019.00173*.

Verma, S., Gautam, V., & Sarkar, A. K. (2019). Improved laser capture microdissection (LCM)-based method for isolation of RNA, including miRNA and expression analysis in woody apple bud meristem. *Planta, 249* (6), 2015-2020.*https://doi.org/10.1007/s00425-019-03127-0*.

Wang, C., Wang, J. & Jiang, H. (2009). Morphological and structural characteristics of forest stems of Pinus yunnanensis and its relatives in different habitats. *Western Forestry Science,* 38**,**23-28.*https://doi.org/10.16473/j.cnki*.

Wang, H., Cui, K., Shao, S., Liu, J., Chen, H., Wang, C., Wu, H., Yang, Z., Lu, Q., Jones, K. K., & Chen, X. (2017). Molecular response of gall induction by aphid *Schlechtendalia chinensis* (Bell) attack on Rhus chinensis Mill. *Journal of Plant Interactions, 12* (1), 465-479.*https://doi.org/10.1080/17429145.2017.1392627*.

Wang, L., Hart, B. E., Khan, G. A., Cruz, E. R., Persson, S., & Wallace, I. S. (2020). Associations between phytohormones and cellulose biosynthesis in land plants. *Annals of Botany, 126* (5), 807-824.*https://doi.org/10.1093/aob/mcaa121*.

Wang, L., Liu, Y., Liu, C., Ge, C., Xu, F., & Luo, M. (2021). Ectopic expression of *GhIQD14* (Cotton *IQ67* domain-containing protein 14) causes twisted organ and modulates secondary wall formation in *Arabidopsis* . *Plant Physiology and Biochemistry, 163* (4), 276-284.*https://doi.org/10.1016/j.plaphy.2021.04.004*.

Weizbauer, R., Peters, W. S., & Schulz, B. (2011). Geometric Constraints and the Anatomical Interpretation of Twisted Plant Organ Phenotypes. *Frontiers in Plant Science, 2* (62), 1-8.*https://doi.org/10.3389/fpls.2011.00062*.

Xiao, Z., Zhang, Y., Liu, M., Zhan, C., Yang, X., Nvsvrot, T., Yan, Z., & Wang, N. (2020). Coexpression analysis of a large-scale transcriptome identified a calmodulin-like protein regulating the development of adventitious roots in poplar. *Tree Physiology, 40* (10), 1405-1419.*https://doi.org/10.1093/treephys/tpaa078*.

Xin, X., Lei, L., Zheng, Y., Zhang, T., Pingali, S. V., O'Neill, H., Cosgrove, D. J., Li, S., & Gu, Y. (2020). Cellulose synthase interactive1- and microtubule-dependent cell wall architecture is re-

quired for acid growth in Arabidopsis hypocotyls. *Journal of Experimental Botany, 71* (10), 2982-2994.*https://doi.org/10.1093/jxb/eraa063*.

Xu, Y. (2015). Genetic variation of natural populations in *Pinus yunnanensis* Franch. *Forestry Tree Genetics and Breeding* , 12.

Yang, Q., Wan, X., Wang, J., Zhang, Y., Zhang, J., Wang, T., Yang, C., & Ye, Z. (2020). The loss of function of *HEL* , which encodes a cellulose synthase interactive protein, causes helical and vine-like growth of tomato. *Horticulture Research, 7 .https://doi.org/10.1038/s41438-020-00402-0*.

Ye, X., Huang, H., Wu, F., Cai, L., Lai, N., Deng, C., Guo, J., Yang, L., & Chen, L. (2020). Molecular mechanisms for magnesium-deficiency-induced leaf vein lignification, enlargement and cracking in *Citrus sinensis* revealed by RNA-Seq. *Tree Physiology, 41* (2), 280-301.*https://doi.org/10.1093/treephys/tpaa128*.

Yoshida, T. (1994). Dwarfism in Trifoliate Orange (*Poncirus trifoliata* Raf.), Its Inheritanc and Interaction with GA_3. *Journal of the Japanese Society for Horticultural Science, 63* (1), 23-30.*https://doi.org/10.2503/jjshs.63.23*.

Yua, M., Liua, K., Liu, S., Chen, H., Zhou, L., & Liu, Y. (2016). Effect of exogenous IAA on tension wood formation by facilitating polar auxin transport and cellulose biosynthesis in hybrid poplar (*Populus deltoids* × *Populus nigra*) wood.*Holzforschung, 71* (2), 179-188.*https://doi.org/10.1515/hf-2016-0078*.

Yuan, Y., Mei, L., Wu, M., Wei, W., Shan, W., Gong, Z., Zang, Q., Yang, F., Yan, F., Zhang, Q., Luo, Y., Xu, X., Zhang, W., Miao, M., Lu, W., Li, Z., & Deng, W. (2018). SlARF10, an auxin response factor, is involved in chlorophyll and sugar accumulation during tomato fruit development. *Journal of Experimental Botany, 69* (22), 5507-5518.*https://doi.org/10.1093/jxb/ery328*.

Zhang, K., Yang, D., Zhang, Y., Ellsworth, D. S., Xu, K., Zhang, Y., Chen, Y., He, F., & Zhang, J. (2021). Differentiation in stem and leaf traits among sympatric lianas, scandent shrubs and trees in a subalpine cold temperate forest. *Tree Physiology, 41* (11), 1992-2003.*https://doi.org/10.1093/treephys/tpab049*.

Zhang, L., Yan, P., Shen, C., Zhang, L., Wei, J., Xu, H., Li, X., & Han, W. (2017). Effects of exogenous TIBA on dwarfing, shoot branching and yield of tea plant (*Camellia sinensis* L.). *Scientia Horticulturae, 225* , 676-680.*https://doi.org/10.1016/j.scienta.2017.07.060*.

Zhao, F. Y., Han, X. L., & Zhang, S. Y. (2019). Combined Treatment with Cadmium and Zinc Enhances Lateral Root Development by Regulating Auxin Redistribution and Cell-Cycle Gene Expression in Rice Seedlings.*Russian Journal of Plant Physiology, 66* (4), 597-608.*https://doi.org/10.1134/s1021443719040162*.

Zheng, P., Aoki, D., Matsushita, Y., Yagami, S., Sano, Y., Yoshida, M., & Fukushima, K. (2016). Lignification of ray parenchyma cells (RPCs) in the xylem of *Phellodendron amurense* Rupr.: quantitative and structural investigation by TOF-SIMS and thioacidolysis of laser microdissection cuts of RPCs. *Holzforschung, 70* (7), 641-652.*https://doi.org/10.1515/hf-2015-0120*.

Zheng, T., Li, L., & Zhang, Q. (2018). Advances in research on tortuous traits of plants. *Euphytica, 214* (12), 224.*https://doi.org/10.1007/s10681-018-2306-0*.

Zhou, A., Zong, D., Roga, H., Shen, D., He, R., Tian, B., Xu, Y. & He, C. (2016). AFLP Analysis of Genetic Variation of Pine Yunnan in Different Dry Shapes. *Molecular Plant Breeding,* 14**,**186-194. https://doi.org/10.13271/j.mpb.014.000186.s.

Figure Captions

Figure 1 Variations in height and DBH (diameter at breast height) of*P. yunnanensis* at different growth stages. Lines in different colors indicate straight and twisty *P. yunnanensis* , respectively. Bars represent SE.

Figure 2 Anatomical differences in the stem of straight and twisty*P. yunnanensis* . A 1-year-old *P. yunnanensis* shows clear twisting of the xylem texture after peeling; B-C Growth status of straight and twisty *P. yunnanensis* in the field; D–I Results of paraffin sections, in which D, F, and H represent materials with

straight growth at 30, 60, and 180 days, respectively, while E, G, and I represent materials with twisted growth at 30, 60, and 180 days, respectively; J–M Results of SEM; S180 and T180 represent materials with straight and twisty growth at 180 days, respectively. Bar = 100 μm.

Figure 3 RNA-seq analysis of twisty and straight stem segments of*P. yunnanensis* at different growth stages. A, Transcripts and unigene length distribution; B, Volcano plot of DEGs; C, VENN plot of DEGs involved in twisty versus straight *P. yunnanensis* at different growth stages. D, KEGG enrichment plot of upregulated genes in T180 vs S180; E, KEGG enrichment plot of downregulated genes in T180 vs S180.

Figure 4 MapMan metabolism overview displaying differences in transcript levels (T180 versus S180). The average transcript abundance was transformed to Log2 ratios based on three replicates. The resulting file was loaded into the MapMan Image Annotator module to generate the metabolism overview map. On the logarithmic color scale, blue and red indicate downregulated and upregulated transcripts, respectively.

Figure 5 Heat map of the correlation between twisty and straight*P. yunnanensis* at different growth stages and modules. Each cell contains the corresponding Pearson's correlation coefficient and the p value (in brackets) determined by the groups' eigengene.

Figure 6 DEGs involved in starch and sucrose metabolic pathways during the development of twisty and straight traits in *P. yunnanensis* .*BAM* , beta-amylase; *BGL* , beta-glucosidase; *CBH* , cellulose 1,4-beta-cellobiosidase; *EGase* , endoglucanase;*EXG* , glucan 1,3-beta-glucosidase; *INV* , invertases; and*Susy* , sucrose synthase.

Figure 7 DEGs involved in photosynthetic carbon fixation metabolic pathways during the development of twisty traits in *P. yunnanensis* . *AST* , aspartate aminotransferase; *dmlA* , malate dehydrogenase(decarboxylating); *FBA* , fructose-bisphosphate aldolase; *FBP* , fructose-1,6-bisphosphatase I; *GAPDH* , glyceraldehyde-3-phosphate dehydrogenase; *MDH* , malate dehydrogenase; *PEPCK* , phosphoenolpyruvate carboxykinase;*PGK* , phosphoglycerate kinase; *PRK* , phosphoribulokinase;*XFP* , xylulose-5-phosphate; *XPK* , fructose-6-phosphate phosphoketolase.

Figure 8 DEGs involved in auxin signal transduction and metabolic pathways in the development of stem twisting in *P. yunnanensis* . A, *ARF* , auxin response factor; *BSU1* , serine/threonine-protein phosphatase; *PP2C* , protein phosphatase 2C; *PR-1* , pathogenesis-related protein 1; *SAUR* , small auxin up RNA; *SnRK2* , serine/threonine-protein kinase;*TCH4* , xyloglucosyl transferase; and *TIR1* , transport inhibitor response 1. B, *ABAH* , abscisic acid 8'-hydroxylase;*DHQ/SDH* , 3-dehydroquinate dehydratase/shikimate dehydrogenase;*DXR* , 1-deoxy-D-xylulose-5-phosphate reductoisomerase;*NCED* , 9-cis-epoxycarotenoid dioxygenase; *PGD* , 6-phosphogluconate dehydrogenase; *PIN* , auxin efflux carrier component; and *YUC* , indole-3-pyruvate monooxygenase.

Figure 9 Phenotypic analysis of straight and twisty *P. yunnanensis* after being sprayed with auxin/auxin inhibitors. A: Phenotypes of *P. yunnanensis* 55 days after being sprayed with IAA. B: The plant height monitoring of *P. yunnanensis* sprayed with IAA and the control for 55 days. C: Phenotypes of *P. yunnanensis* 55 days after being sprayed with TIBA. D: The plant height monitoring of *P. yunnanensis* sprayed with TIBA and the control for 55 days. E: Phenotypes of *P. yunnanensis* 55 days after being sprayed with auxinole. F: The plant height monitoring of *P. yunnanensis* sprayed with auxinole and the control for 55 days. G: Phenotypes of *P. yunnanensis* 55 days after being sprayed with distilled water. H: Phenotypes of *P. yunnanensis* 55 days after being sprayed with *P. syringae* . Bars represent ST. The scales represent 1 cm.

Figure 10 Biochemical characteristics of S60 and T60 after hormone spraying. A, Acid invertase (AI); B, PEPC, Phosphoenolpyruvate carboxylase; C, PFK, Phosphofructokinase; D, SS-I, Sucrose synthase decomposition direction; E, SS-II, Sucrose synthase synthesis direction.*, ** and ***indicate differences at 0.05, 0.01 and 0.001 level based on the Student's t -test, respectively. Bars represent ST.

Figure 11 Immunohistochemical analysis of *P. yunnanensis* . CDC2, Cell-division-cycle kinase 2; cFBPase, Cytosolic fructose-1,6-bisphosphatase; PEPCK, PEP carboxykinase; POR, Protochlorophilide oxidoreduc-

tase; RbcL, Rubisco large subunit, form I; SUS1, Sucrose synthase 1. S30, 30-day-old straight *P. yunnanensis* ; S60, 60-day-old straight *P. yunnanensis* ; S180, 180-day-old straight *P. yunnanensis* ; T30, 30-day-old twisty*P. yunnanensis* ; T60, 60-day-old twisty *P. yunnanensis* ; T180, 180-day-old twisty *P. yunnanensis* . Bar = 100 μm.

Figure 12 A–D, Cellulose, lignin, hemicellulose and sucrose contents of straight and twisty *P. yunnanensis* S60, S180, T60, and T180 were compared, and significance was determined by performing a student's*t* -test. *, ** and*** indicate differences at 0.05, 0.01 and 0.001 level, respectively.

Figure 13 qRT-PCR analysis of DEGs in 6 periods (S30, T30, S60, T60, S180, T180). Column and broken line are corresponded to qRT-PCR and FPKM in RNA-seq, respectively. *ARF* , auxin response factor; *BAM* , beta-amylase; *BGL* , beta-glucosidase; *CBH* , cellulose 1,4-beta-cellobiosidase; *CDC2* , cell-division-cycle kinase 2;*cFBPase* , cytosolic fructose-1,6-bisphosphatase; *FBA* , fructose-bisphosphate aldolase; *FBP* , fructose-1,6-bisphosphatase I; *INV* , invertases; *PEPCK* , PEP carboxykinase; *PGK* , phosphoglycerate kinase; *PIN* , auxin efflux carrier component;*POR* , protochlorophilide oxidoreductase; *RbcL* , rubisco large subunit, form I; *SAUR* , small auxin up RNA; *SUS1* , sucrose synthase 1; *TIR1* , transport inhibitor response 1;*XFP* , xylulose-5-phosphate; *YUC* , indole-3-pyruvate monooxygenase. Bars represent ST.

Figure 14 Schematic diagram showing the formation pattern of straight and twisty *P. yunnanensis* . This model was constructed using DEGs involved in phytohormone synthesis and signal transduction, and sucrose metabolism associated with photosynthesis. *ARF* , auxin response factor; *CBH* , cellulose 1,4-beta-cellobiosidase; *FBA* , fructose-bisphosphate aldolase; *FBP* , fructose-1,6-bisphosphatase I; *INV* , invertases; *PGK* , phosphoglycerate kinase;*PIN* , auxin efflux carrier component; *POR* , protochlorophyllide oxidoreductase; *PRK* , phosphoribulokinase;*RbcL* , rubisco large subunit, form I; *SAUR* , small auxin up RNA; *Susy* , sucrose synthase; *TIR1* , transport inhibitor response 1; *XFP* , xylulose-5-phosphate; *XPK* , fructose-6-phosphate phosphoketolase.

Table Captions

Table 1 Segregation for growth habit in *P. yunnanensis*

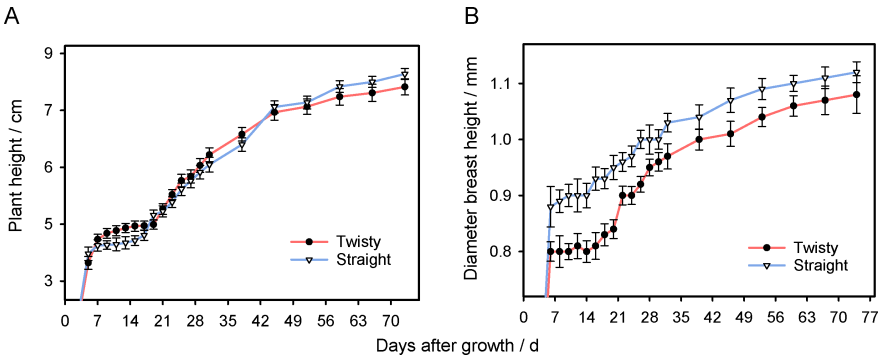

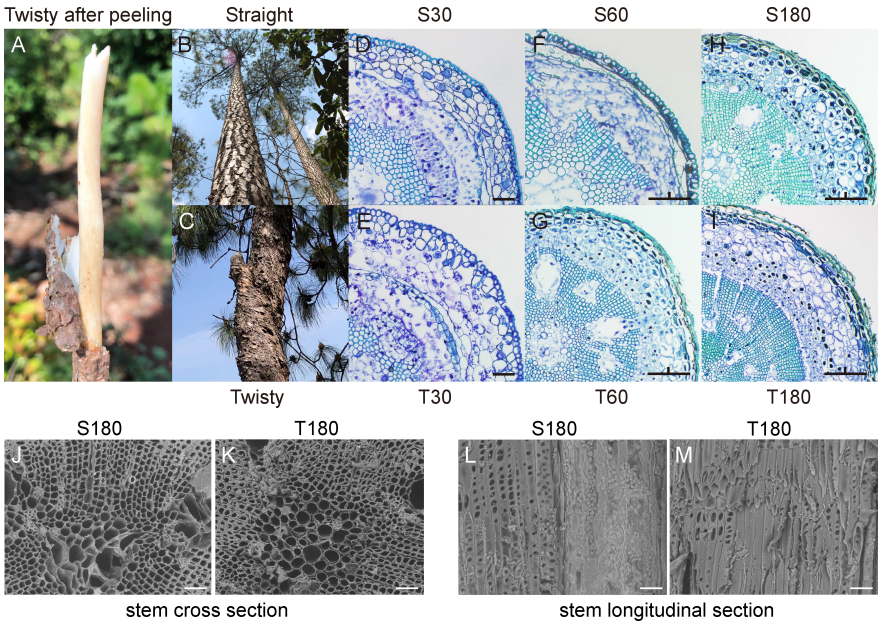

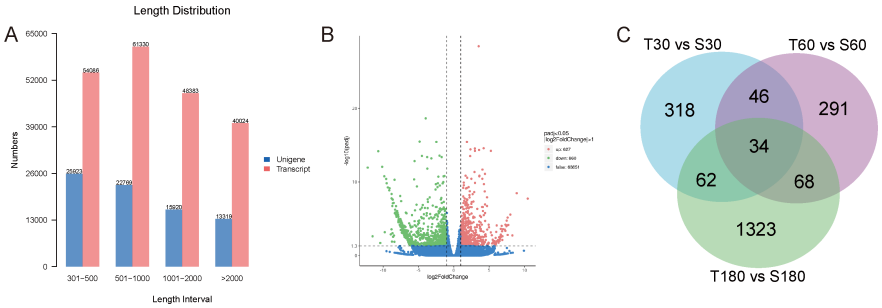

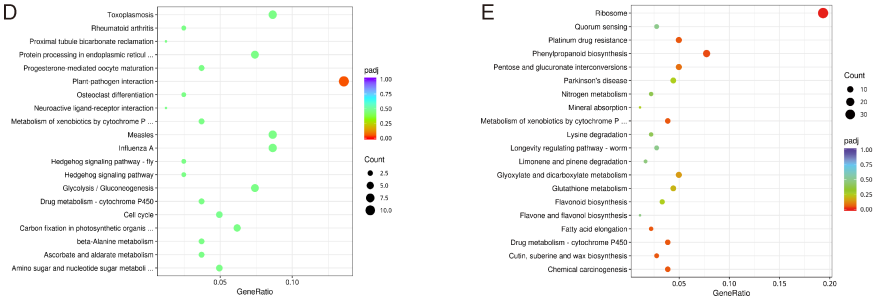

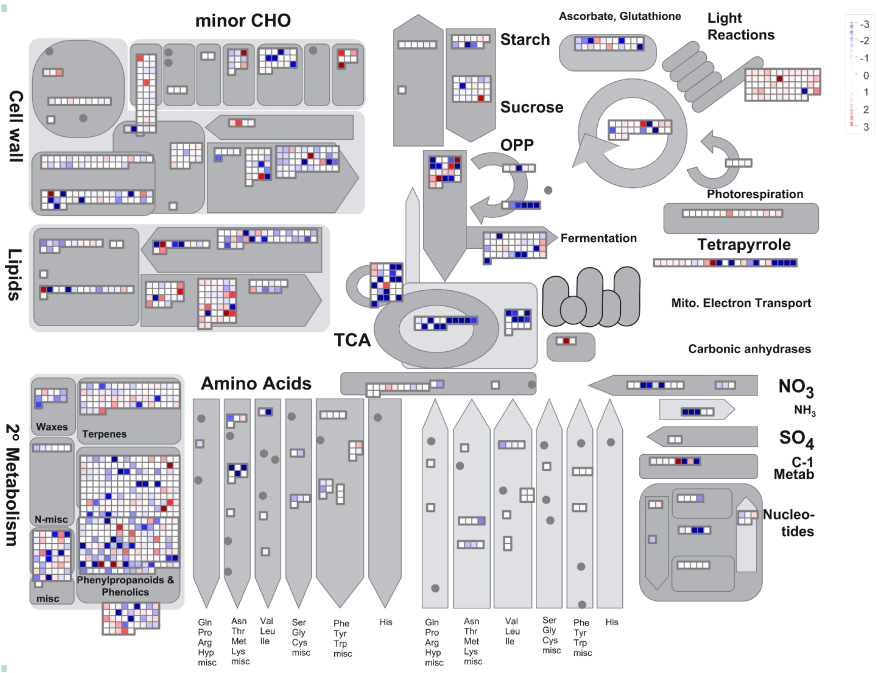

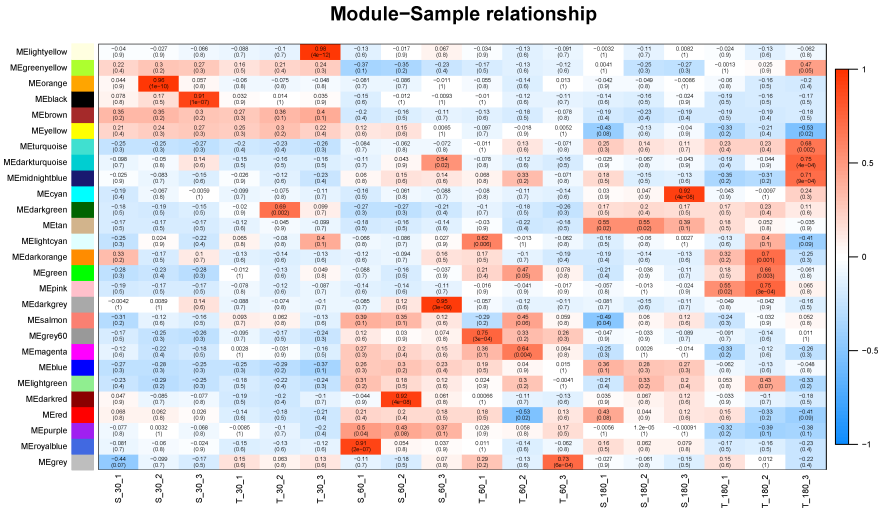

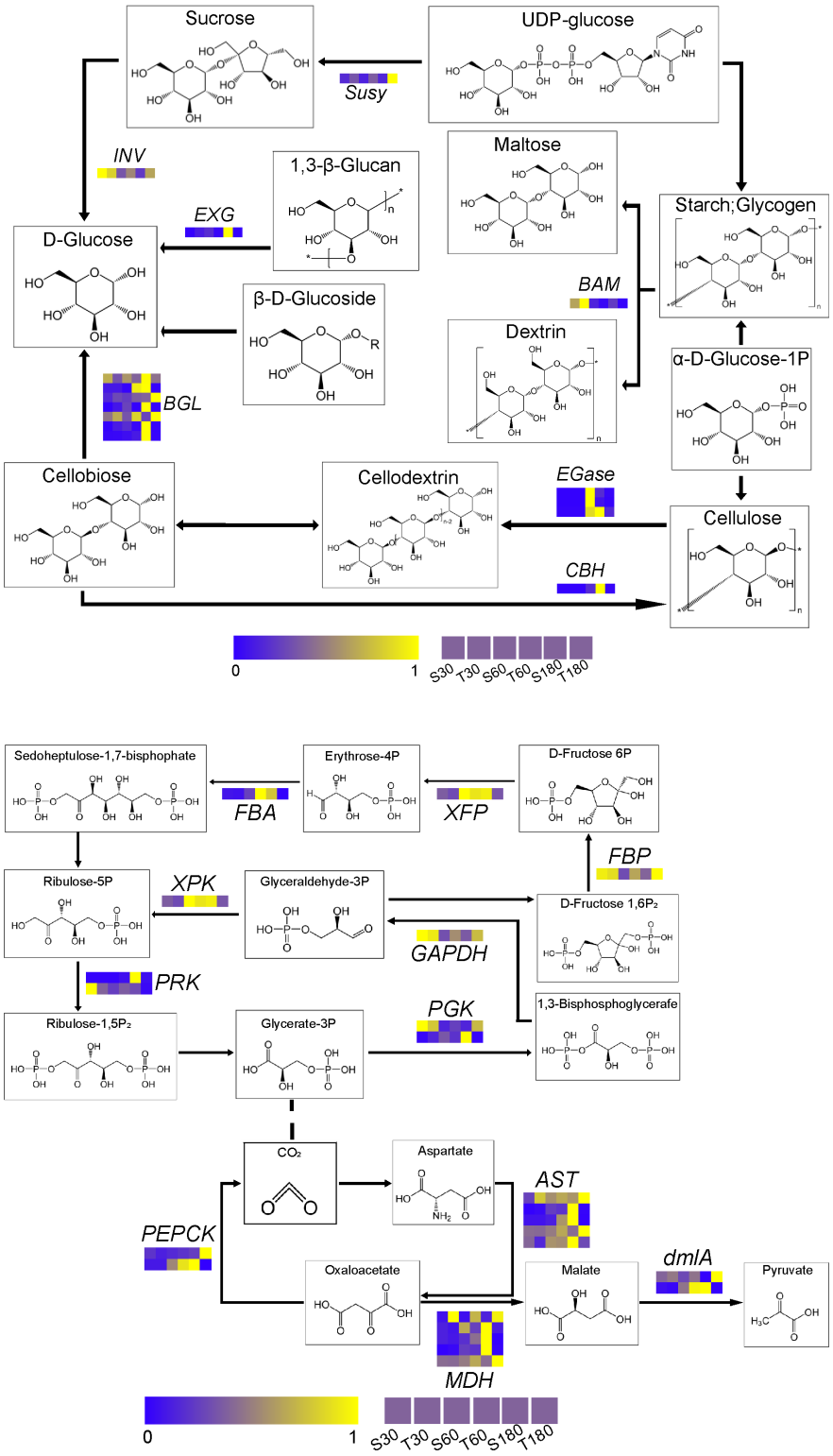

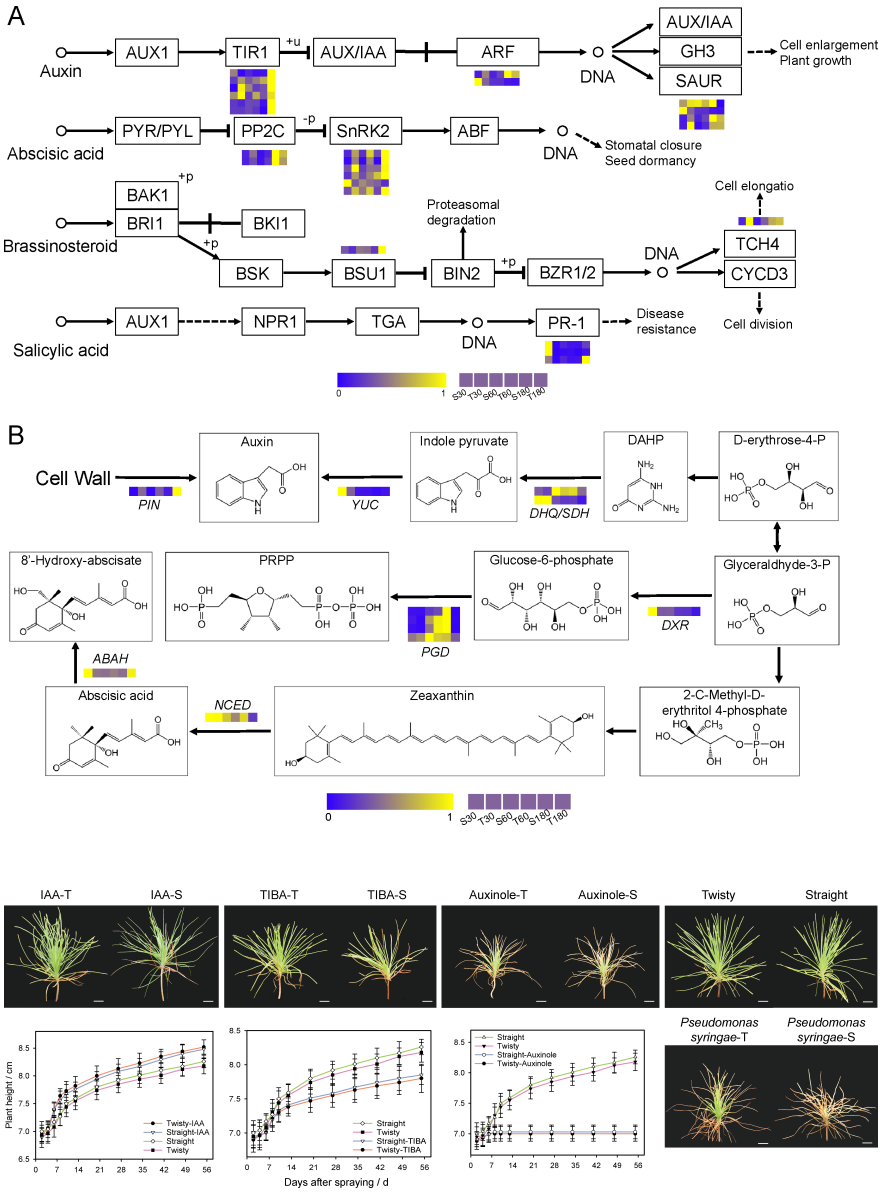

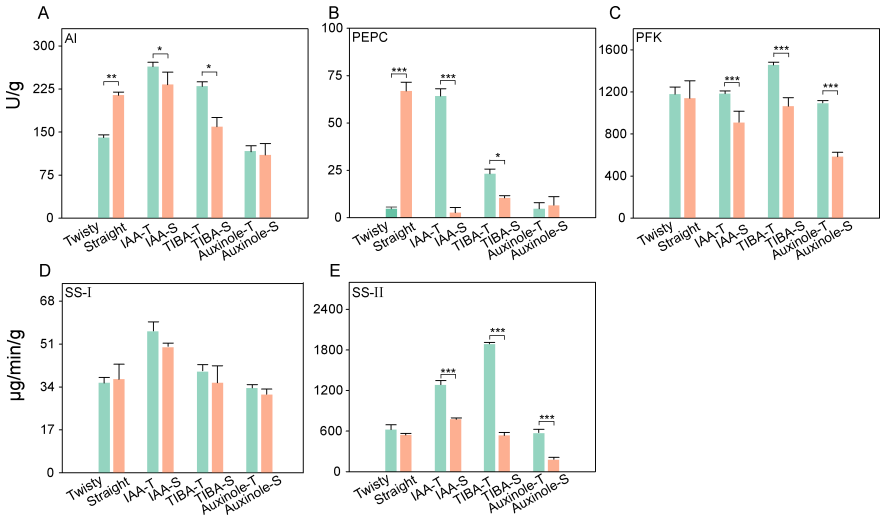

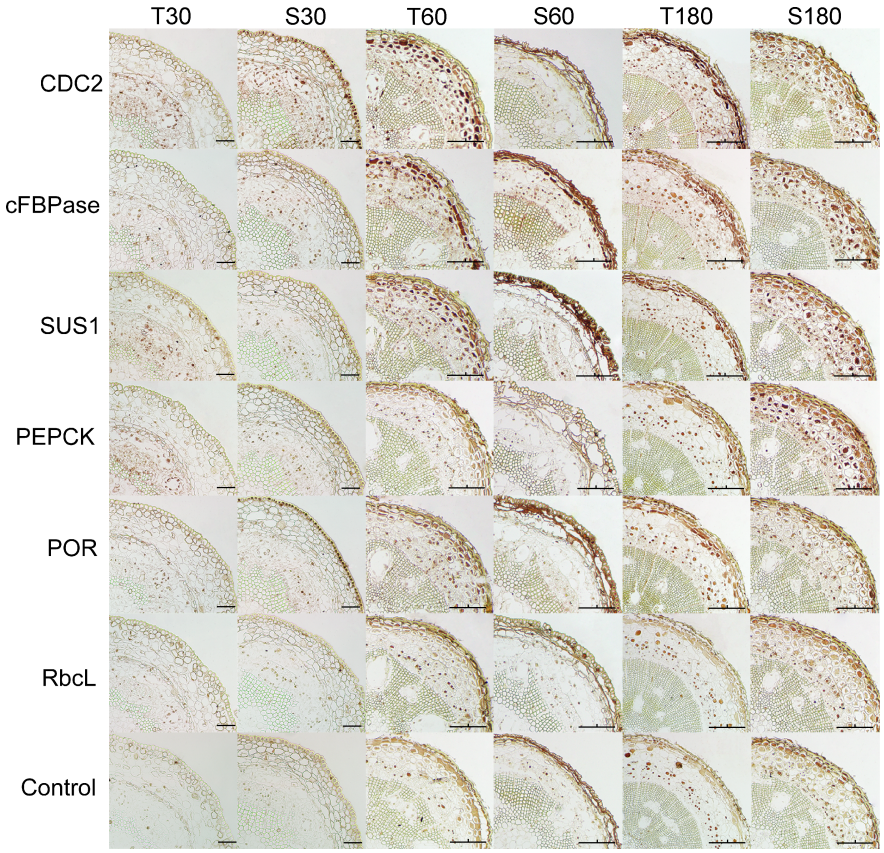

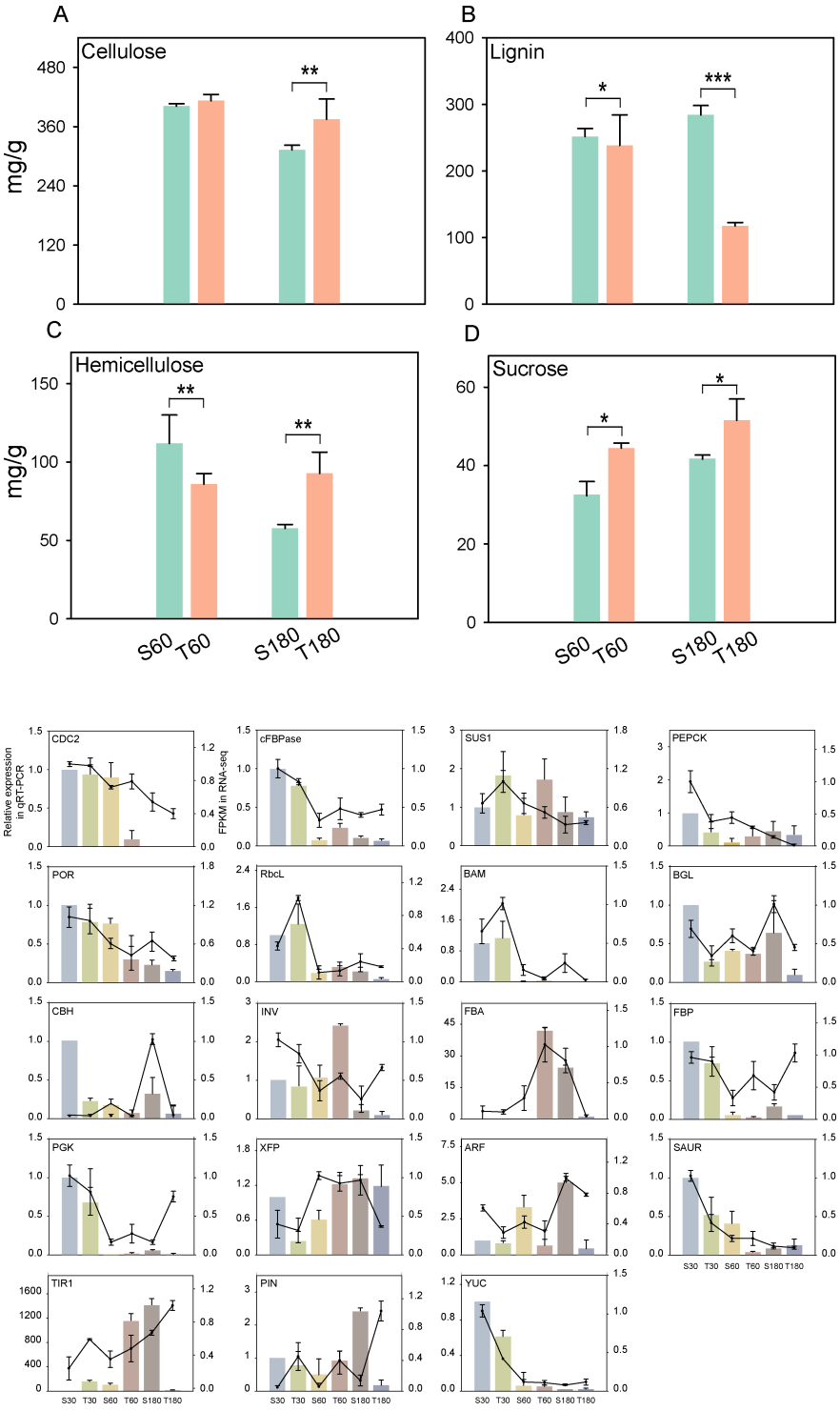

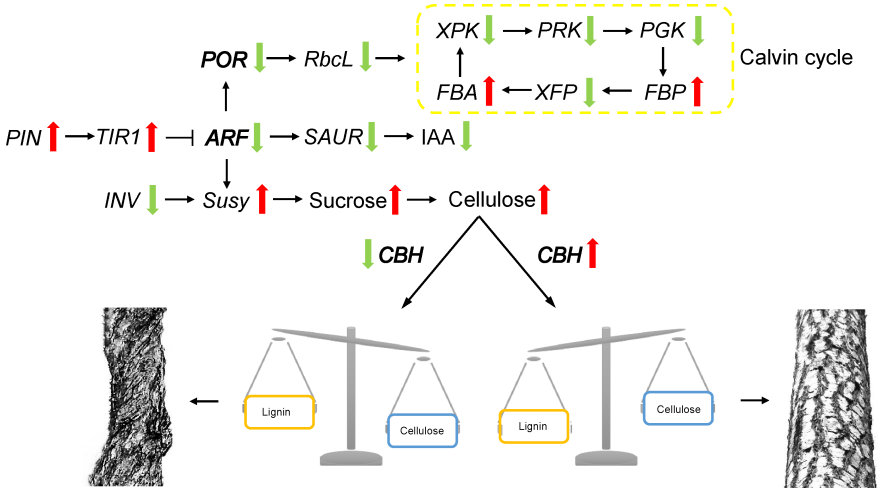

Hosted file

Table 1.docx available at https://authorea.com/users/513570/articles/589711-the-cellulose-lignin-balance-affects-the-twisted-growth-of-yunnan-pine-trunk